

On the Nature of the NGC 1275 System

Christopher J. Conselice¹, John S. Gallagher, III²

Department of Astronomy, University of Wisconsin, Madison, 475 N. Charter St. Madison, WI,
53706-1582: consel@stsci.edu, jsg@astro.wisc.edu

Rosemary F.G. Wyse²

Department of Physics and Astronomy, Johns Hopkins University, Baltimore, MD. 21218;
wyse@tarkus.pha.jhu.edu

Subject headings: galaxies: clusters: individual (Perseus) - galaxies: individual (NGC 1275) -
galaxies: formation - galaxies: interactions - galaxies: evolution

Accepted to the Astronomical Journal

ABSTRACT

Sub-arcsecond images, taken in B, R, and H α filters, and area spectroscopy obtained with the WIYN 3.5-m telescope provide the basis for an investigation of the unusual structures in the stellar body and ionized gas in and around the Perseus cluster central galaxy, NGC 1275. Our H α filter is tuned to gas at the velocity of NGC 1275, revealing complex, probably unresolved, small-scale features in the extended ionized gas, located up to $50h_{100}^{-1}$ kpc from NGC 1275. The mean H α surface brightness varies little along the outer filaments; this, together with the complex excitation state demonstrated by spectra, imply that the filaments are likely to be tubes, or ribbons, of gas. The morphology, location and inferred physical parameters of the gas in the filaments are consistent with a model whereby the filaments form through compression of the intracluster gas by relativistic plasma emitted from the active nucleus of NGC 1275. Imaging spectroscopy with the Densepak fiber array on WIYN suggests partial rotational support of the inner component of low velocity ionized gas. Our broad-band data is used to derive color maps of the stellar distribution, and also to investigate asymmetries in the stellar surface brightness. We confirm and extend evidence for features in the stellar body of NGC 1275, and identify outer stellar regions containing very blue, probably very young, star clusters. We interpret these as evidence for recent accretion of a gas-rich system, with subsequent star formation. Other star clusters are identified, some of which are possibly associated with the high velocity 8200 km s⁻¹ emission line system, being in the same projected location. We suggest that two main processes, which may be causally connected, are responsible for the rich phenomenology of the NGC 1275 system – NGC 1275 experienced a recent merger/interaction with a group of gas-rich galaxies, and recent outflows from its AGN have compressed the intracluster gas, and perhaps the gas in the infalling galaxies, to produce a complex web of filaments.

¹Space Telescope Science Institute, 3700 San Martin Drive, Baltimore MD, 21218.

²Visiting Astronomer, Kitt Peak National Observatory, National Optical Astronomy Observatories, which is operated by the Association of Universities for Research in Astronomy, Inc. (AURA) under cooperative agreement with the National Science Foundation.

1. Introduction

NGC 1275 (Perseus A, 3C 84) is one of the most unusual early-type galaxies in the nearby universe and contains an example of almost every known extragalactic phenomenon. However, several of its basic observed features still remain a mystery. NGC 1275 is located at the center of the Perseus cluster and resembles a normal elliptical galaxy on low-resolution plates (Hubble 1931). Humason (1932) and later Seyfert (1943) discovered strong emission lines in NGC 1275. Later, Minkowski (1955) found two distinct emission line systems towards NGC 1275; a high velocity (HV) component at $V = 8200 \text{ km s}^{-1}$, and a low velocity (LV) one at $V = 5200 \text{ km s}^{-1}$. The stellar radial velocity of NGC 1275 is $5264 \pm 11 \text{ km s}^{-1}$ (Huchra, Vogeley & Geller 1999) while the velocity dispersion of the Perseus cluster is 1277 km s^{-1} (Struble & Rood 1991). The puzzling nature of NGC 1275 was compounded by the discovery of an extensive array of emission line filaments projecting away from the central galaxy (Minkowski 1957; Lynds 1970). The origin of these features is still being debated (e.g., McNamara, O’Connell, & Sarazin 1996; Sabra, Shields, & Filippenko 2000).

The HV system is located to the north and north-west direction of the nucleus (Burbidge & Burbidge 1965; Rubin et al. 1977). The presence of HI and X-ray absorption clearly places this gas in front of the nucleus, where it is difficult to explain as a simple outflow (De Young, Roberts & Saslaw 1973; van Gorkom & Ekers 1983; Fabian et al. 2000). Thus, this object could be associated with a foreground late-type spiral falling into the cluster (Rubin et al. 1977; Kent & Sargent 1979; Boroson 1990; Caulet et al. 1992).

Despite appearing as an elliptical galaxy on photographic plates, particularly in the red, NGC 1275 has relatively blue central colors (e.g. van den Bergh 1977), massive young star clusters (Shields & Filippenko 1990; Holtzman et al. 1992), an A-type integrated blue region spectrum (Wirth et al. 1983) and internal sub-structures (Holtzman et al. 1992). Massive, short-lived stars are forming in NGC 1275, that perhaps originate from gas accretion induced in a cooling flow (e.g. Cowie et al. 1980; Sarazin & O’Connell 1983), or their formation is induced from a galaxy merger independent of the high-velocity system (Holtzman et al. 1992).

Is star formation related to the filamentary structure of ionized gas seen in Figure 1? Fabian and Nulsen (1977) interpreted these filaments as a result of accretion of cooling intracluster medium (ICM) gas. Pioneering digital optical spectroscopy yielded emission line intensities of the filaments that are consistent with either shocked gas or gas photo-ionization by the inferred active BL Lac nucleus in NGC 1275 (Kent & Sargent 1979). Recently Sabra, Shields, and Filippenko (2000) found that neither shocks nor photoionization alone can reproduce the observed emission line intensity ratios in the inner part of the galaxy.

In this paper, we present high-resolution images, integral field and long-slit spectroscopy of NGC 1275 taken with the WIYN 3.5m and KPNO 4m telescopes. We present evidence that the low-velocity ionized gas within NGC 1275 is partially supported by rotation, consistent with a rotating gas disk as seen in emission from CO (Bridges & Irwin 1998). Properties of the filament system as a whole appear to be consistent with the model proposed by McNamara, O’Connell, and Sarazin (1996; hereafter MOS96). They suggested that the ionized filaments originate from interactions between the hot ICM and the relativistic plasma responsible for the radio source (see also Böhringer et al. 1993; Heinz, Reynolds & Begelman 1998; Churazov et al. 2000). Instabilities should occur in the compressed and cooling ICM as it sinks through the dilute relativistic plasma, possibly in a manner similar to that of ionized gas filaments in the Crab nebula (Hester et al. 1996). This process could lead to the production of a radial system of filaments.

We employ several methods to investigate the structure of the stellar body of NGC 1275, including B–R color maps, and the removal of symmetric, or smooth light, components to reveal complex or asymmetric features. We find more evidence for low amplitude, blue stellar shells or ripples in the main body of the galaxy (cf., Holtzman et al. 1992; Carlson et al. 1998) and blue star clusters possibly not associated with the LV H α emission. NGC 1275 clearly suffered a recent, significant perturbation, probably induced by some type of merger, which may be the source of the system’s peculiarities.

Section 2 of the paper describes the observations, Section 3 is an analysis of the data, Section 4 is an interpretation, while Section 5 gives a summary. Throughout this paper we use the following terminology: ‘low-velocity (LV) system’ denotes the 5200 km s $^{-1}$ ionized gas around NGC 1275, ‘high-velocity (HV) system’ denotes the 8200 km s $^{-1}$ ionized gas system localized to the northwest of NGC 1275, and ‘NGC 1275’ refers to the central galaxy (redshift 5264 km s $^{-1}$) of the Perseus cluster without regard to the LV or HV ionized gas components. For quantities not expressed in terms of h $_{100}^{-1}$, we adopt a distance to the Perseus cluster of 70 Mpc.

2. Observations

The images used in this paper were taken in 1998 November with the WIYN 3.5m telescope located at the Kitt Peak National Observatory near Tucson, AZ. CCD images were obtained with a 2048 2 -pixel thinned S2kB device, producing data with a scale of 0.2 arcsec per pixel. The field of view of each image is 6.8 \times 6.8 arcmin 2 . NGC 1275 and the surrounding region of the core of the cluster were observed in the broadband R and B filters, as well as a narrow band H α filter centered on the radial velocity of the LV component (KPNO filter KP1495 with central wavelength 6690 \AA and FWHM of 77 \AA) which excludes most of the emission from the HV system.

Exposure times for the R images were 2 \times 800 sec, while the exposure times for the B images were 3 \times 700 sec, and the H α images had exposure times of 3 \times 800 sec. The average seeing for all the combined images is 0.6''–0.8''. Conditions were photometric, allowing magnitudes to be calibrated using Landolt standard star fields. These images are part of a larger program to study the galaxy populations in the Perseus Cluster (e.g., Conselice, Gallagher & Wyse 2001). A total of 231 arcmin 2 of area in the core of the Perseus cluster was imaged during this run.

We removed the continuum from the combined 2400s H α image by subtracting a R band image normalized with respect to field stars, with an estimated accuracy of 7%. We calibrated the H α fluxes with the spectrophotometric standard SA 29-130, a DA white dwarf with spectrophotometry by Oke (1974). We convolved the spectrum of SA 29-130 with the filter transmission function to obtain a calibrated flux, yielding 2.6 \times 10 $^{-15}$ erg s $^{-1}$ cm $^{-2}$ /(count/s) corrected for Galactic extinction. The total H α luminosity of the LV component of NGC 1275 in the H α + [NII] emission lines is then 4.9 \times 10 42 erg s $^{-1}$. No significant H α emission is present in locations beyond the NGC 1275 filaments. We correct for Galactic extinction using E(B–V) = 0.17 and A $_B$ = 0.71, A $_R$ = 0.40 (Burstein & Heiles 1984).

Integral field spectroscopy of the center of NGC 1275 was obtained with the Densepak fiber array (Barden & Wade 1988) on WIYN during November 1998. Densepak contains 94 optical fibers arranged in an area 45'' \times 27'', with each fiber separated by 4''. The spectral resolution was 3 \AA (\sim 140 km s $^{-1}$ at H α). Three 900 second exposures were taken, and later reduced by the IRAF task DOHYDRA. A CuAr comparison source was used to produce a wavelength calibration. The variable and unpredictable flux throughput of each fiber makes spectrophotometry with Densepak unreliable. Accordingly, we derive only

an integral field velocity map from the fiber spectra. We measure and fit the low-velocity $H\alpha$ line in each fiber to obtain a central wavelength and radial velocity, which we use to produce a velocity field.

Additional long slit spectroscopy was obtained with the RC spectrograph on the KPNO 4m Mayall telescope on 1999 October 2 for spectrophotometric purposes. We chose three different filaments around the center and $2'$ from NGC1275. The KPC-10A grating was used, giving a wavelength coverage of 4000 \AA with a $2'' \times 300''$ slit, and 7 \AA resolution. Two 750s exposures were taken in each of the three different areas of the ionized filaments of NGC1275. These data were reduced with the KPNO long-slit tools, undergoing a trim, extraction and sky subtraction. The spectra were then calibrated in wavelength with an FeAr lamp and flux calibrated by the standard BD+28 4211. The useful wavelength range of the spectra is 3700 \AA to 7800 \AA . We corrected the spectra for interstellar extinction using the method of Cardelli, Clayton and Mathis (1989), using $E(B-V) = 0.17$.

3. Results

3.1. $H\alpha$ Structure of the Low-Velocity Ionized Gas

3.1.1. *The Forms and Origin of the Ionized Gas Filaments*

One of the most remarkable properties of NGC 1275 is the intricate array of LV $H\alpha$ filaments that can be seen in Figures 1-6. Our angular resolution of $0.6\text{-}0.8''$ corresponds to $150\text{-}200h_{100}^{-1} \text{ pc}$ at the distance of NGC 1275, and structures exist in these filaments down to this resolution limit. Following the description of the NGC 1275 filaments by Lynds (1970), extended $H\alpha$ emission has been observed surrounding other central cluster galaxies (e.g., Heckman 1981, Heckman et al. 1989). In some cases filamentary morphologies similar to that in NGC 1275 are found, as in *Hubble Space Telescope* images of the central cD galaxy in the cluster Abell 2597 (Koekemoer et al. 1999).

The filaments cover a total linear distance of nearly $100h_{100}^{-1} \text{ kpc}$ from north to south. These extend from a central system of filamentary ionized gas in NGC 1275 that is elongated over approximately $\approx 40h_{100}^{-1} \text{ kpc}$ in the east-west direction, along the major axis of the stellar part of the galaxy. The large north-south extent of $100 h_{100}^{-1} \text{ kpc}$ occurs for only a small number of thin, largely unresolved filaments (Figures 2 & 5). Figure 7 shows both the surface brightness profile of the $H\alpha$ emission and its projected filling factor. Despite the fact that the filling factor declines significantly after $\sim 4 \text{ kpc}$, the annular brightness of the filaments remains high.

There are two major forms of ionized gas structures around NGC 1275 - radial and tangential filaments. The radial types point towards the center of NGC 1275; while tangential features usually, but not always, are located at the outer extreme of the $H\alpha$ emitting gas in any particular location. The tangential filaments curve around the galaxy and are concave towards its center. How these two types of filaments relate to each other and to the intergalactic medium around NGC 1275 provides insights into the origin of the ionized gas. Figures 3 and 4 show examples of radial and tangential filaments, which can be seen in abundance throughout the filament system in Figures 1 and 2. The east-west axis of NGC 1275 is less extended in $H\alpha$ gas, and shows a predominance of tangential filaments (Figure 4). Figure 3 illustrates a remarkable filament that remains radial for 30 kpc before folding backwards. The smooth, very elongated morphologies of the filaments suggest that magnetic fields could play a part in defining their structures, as they do in the smaller Crab Nebula ionized filament system (Hester et al. 1996). In fact, some form of additional support, such as magnetic fields, is likely needed to explain the structures of these filaments. For a temperature

of 10^4 K, the filaments will have an average internal random motion $\sim 10 \text{ km s}^{-1}$, giving a lifetime \sim width/velocity = $0.5 \text{ kpc}/10 \text{ km s}^{-1} = 50 \text{ Myrs}$. Either the filaments are supported by processes that allow them to survive more than 50 Myrs, or they are continuously being reformed.

Since we probably have not completely resolved most filaments, we are thus likely underestimating their surface brightnesses. The evolution of filaments near the center of NGC 1275, which might be more compressed, could be quite complex. It is possible that compression and instabilities operate in tandem, as in the Crab nebula (e.g., Hester et al. 1996). Features such as the long linear structure of ionized filaments extending to the north could be the remnants of ICM gas that was displaced by a northward non-thermal radio jet (see Figure 6) that may have been more intense in the past (Pedlar et al. 1990, MOS96, Blundel, Kassim, & Perley 2000). Figure 6 displays the contours from a 1320 MHz VLA radio map, from Pedlar et al. (1990), over the $\text{H}\alpha$ + continuum image of the central parts of NGC 1275. This Figure shows the opposite major axis directions of the two components. In §4.2 we discuss the MOS96 model for filament production in interactions between relativistic plasma outflows from NGC 1275 and the ICM.

The complex filament morphologies lead us to ask what is the true distribution of the $\text{H}\alpha$ gas around NGC 1275. Do the filaments have tubular structures, or are they extended sheets between ionization and shock fronts, possibly along the edges of expanding bubbles? The surface brightnesses of individual filaments are relatively constant over 50 kpc. For example, the large radial filament at the base of the ‘horseshoe’ in Figure 3 has $1.0 < I(\text{H}\alpha + [\text{N II}]) / (10^{-15} \text{ erg s}^{-1} \text{ cm}^{-2} \text{ arcsec}^{-2}) < 6$, while a similar range is found along the very extended northern filaments (Figure 5; Table 1). The filaments often have high contrast with respect to their surroundings, again suggesting a relatively compact physical structure. Table 1 lists the fluxes and intensities of the emission line regions labeled in Figure 5, measured using a $1''$ circular aperture, relative to a local sky measurement.

The near constant surface brightnesses, large linear extent of the northern filaments, and small angular sizes of the radial filaments all imply that they are tubes or compact ribbons of ionized gas, and not projected edges of large bubbles. Further support for the filament interpretation comes from the presence of localized, unresolved high surface brightness areas. These ‘knots’ could be examples of filaments seen end on, especially in the central part of the filament system (see Figure 4 & 5 and entries 28 - 38 in Table 2 for examples), a similar phenomenon is observed in the Crab nebula (see Hester et al. 1996). However, some knots are far out in the system where an end-on projection is less likely; these could be locations where the volume emissivity is locally enhanced, e.g., due to high electron densities or more intense heating of the gas. These ionized knots, labeled as hexagons in Figure 5, mostly have $\text{H}\alpha$ fluxes $\sim 10^{-14} \text{ erg s}^{-1} \text{ cm}^{-2}$. Some of these could also be HII regions.

The tangential filaments also present an interesting picture. When curvature is present, the filaments close in around NGC 1275; an outstanding example is the ‘horseshoe’ located to the northwest of NGC 1275 (Figure 3). This pattern is commonly associated with an *outward* displacement of gas; the loops could mark the edges of expanding regions where gas has been compressed and cooled. The relationship between the location of the LV system ionized filaments, disturbed X-ray emitting gas, and the non-thermal radio source all are consistent with the ionized gas forming where the relativistic plasma recently displaced the hot ICM (Böhringer et al. 1993; Churazov et al. 2000; see §4.1). It is not clear how these concentric ionized features could be produced via an inward moving cooling flow, unless they represented regions where the flow was decelerated by an outward pressure, a model that is conceptually the same as that for an expanding source.

The widths of the filaments vary between $> 0.5 h_{100}^{-1} \text{ kpc}$ in clumps of material, to unresolved features with sizes of $< 165 h_{100}^{-1} \text{ pc}$ further out in the cluster. Any explanation for their origin must account for

these small relative widths of the filaments in comparison to their very long lengths (ratio width/length > 100 , especially at $50h_{100}^{-1}$ kpc, the largest distance from the center of NGC 1275 where filaments are seen).

A simple model based on the measured $H\alpha$ surface brightnesses of the filaments (corrected for Galactic extinction and assuming that about half the flux in the filter is from [N II]) indicate lower bound electron densities of $\geq 10 \text{ cm}^{-3}$. The filaments are then much denser than the surrounding ICM ($n \sim 10^{-2} \text{ cm}^{-3}$) or relativistic plasma, thus a sinking instability could operate. The pressure of these filaments is then $\geq 10^5 \text{ K cm}^{-3}$ for an electron temperature of $\sim 10^4 \text{ K}$. This is below the pressure of the ICM, 10^6 K cm^{-3} , thus the filaments could be experiencing dynamic compression. The inferred presence of a cooling flow (e.g., Fabian et al. 1981) would show that the ICM is not in perfect hydrostatic equilibrium, which could lead to pressure variations over large radial scales, such as the extent of the filaments. However, the [SII] doublet line ratios from spectra (Heckman et al. 1989; Sabra et al. 2000), while covering only a few locations, indicate higher mean electron densities by as much as a factor of 10, in which case the pressure in the filaments is close to that of the ICM. This also would imply a low volume filling-factor for the ionized gas within the filaments.

3.1.2. Photoionization

Shocks or non-thermal radiation from the AGN at the center of NGC 1275 are the most popular explanations for the ionization source of the filaments (Kent and Sargent 1979, Heckman et al. 1989). Others have tried to account for the high ionization flux by a merger between the HV and LV velocity components (Hu et al. 1983), or processes associated with the ICM, such as X-ray photoionization or heating by magnetic reconnections (Heckman et al. 1989, Sabra et al. 2000). However, as emphasized by Sabra et al. none of these mechanisms readily lead to the observed emission line intensity ratios in the filaments.

Figure 7 presents another way to test ionization models. We plot the observed surface brightness profile of the $H\alpha$ flux around NGC 1275 and compare it with the predictions of a simple central source photoionization model, where the rate of ionization equals the rate of recombinations. We assume for the purposes of this plot a distribution of HI that falls off quadratically with spatial distance from the center; the actual form we adopt is not important here since, as can be understood from Figure 7, unless the HI is of uniform density, an unlikely case, this model fails to provide an explanation for the observed $H\alpha$ distribution.

The observed H-alpha intensity profile, in elliptical apertures, centered on NGC 1275 is indicated in red in Figure 7. The result depends sensitively on sky subtraction and thus becomes rather noisy at large radii. The dashed line shows the predicted flux from an isotropic central ionization source, normalized³ at $R = 0$, without any radiative losses other than r^{-2} dimming. This is an *upper* limit to any isotropic central ionization source.

There is a clear shortfall in the model predictions at large radii. This is compounded by the fact that the decline in observed mean intensity is due in large part to a decline in projected filling factor, as shown by the blue curve and right-hand scale in Figure 7, and not in the decline in the mean intensity of

³R denotes the projected radius, while r is the physical radius.

an emitting filament. From Table 1 we see that the mean brightness of typical filaments drops by only a factor of a few between the inner and outer regions of the filament system. Dust could be affecting the distribution of $H\alpha$ flux, but not to the extent seen in Figure 7 since the dust is largely localized near the HV system (see the B–R color map in Figure 8 and Keel & White 2001).

The $H\alpha$ surface brightness in the filaments is nearly always significantly higher, sometimes well over a factor of ~ 100 , than that predicted by a central ionization source model. If the source were beamed, this problem might be avoided, but it is not clear how a beamed photoionization source could power the extensive system of ionized filaments surrounding NGC 1275. Furthermore, the presence of bright, compact emission knots outside of the inner filament system is difficult to understand in any model with a central source of photoionization. Hence we conclude, in agreement with Heckman et al. (1989), that the AGN at the center of NGC 1275 is unable to ionize the filaments, and it is likely that the ionization source, while not a pure shock, is physically associated with the filaments (see also Sabra et al. 2000).

3.2. Star Clusters and Stellar Features

The nature of young star clusters associated with NGC 1275 has been widely discussed, beginning with the discovery of HII regions by Shields & Filippenko (1990) and becoming more vigorous following the first *HST* imaging of this system by Holtzman et al. (1992). Holtzman et al. (1992) characterized a population of blue, possibly young, clusters near the core and suggested that some of these have sizes and stellar masses which would allow them to evolve into globular star clusters. Later studies measured physical parameters of these clusters, such as age and luminosity, to determine the star and cluster formation rate, and constrain the physics behind their formation, e.g., star formation induced from galaxy mergers, or cooling flows (Richer et al. 1993; Norgaard-Nielsen et al. 1993; Faber 1993; Brodie et al. 1998; Carlson et al. 1998).

The spectra and colors of the clusters suggest rather short-lived epochs of cluster formation, rather than the continuous formation expected in cooling flow models (e.g., Holtzman et al. 1992; Carlson et al. 1998; Brodie et al. 1998). Other observations and studies go further, interpreting the narrow range of colors as implying that these clusters formed through merger events (Holtzman et al. 1992; Faber 1993; Carlson et al. 1998). This conclusion has been disputed based on other photometric studies (e.g., Richer et al. 1993) that find a range of colors. The accuracy of the photometry has however been debated in the literature (Faber 1993; Brodie et al. 1998). The presence of young objects is compellingly demonstrated by the WFPC2 photometry of Carlson et al. (1998), who find a bimodal distribution of cluster colors with a population of blue clusters with colors $B-R \approx 0.3 \pm 0.2$.

Since some uncertainties remain regarding photometry for the brightest cluster complexes, we have measured B and R magnitudes for the brighter clusters in the main body and for the asymmetric stellar features in NGC 1275. We also present the first results for objects in the blue star forming extensions of NGC 1275. The clusters measured are labeled in Figures 8 and 9, and are listed in Table 2. These specific clusters are among the brightest in the NGC 1275 system. These clusters are not located in regions of strong emission from ionized gas, which would contribute extra light to both the B and R bands. Line emission is thus unlikely to be a substantial source of error in our colors, which are dominated by uncertainties in the complex continuum backgrounds. We therefore do not attempt to correct for any line emission associated with the individual clusters.

Accurate photometry of the NGC 1275 star clusters is highly compromised by the ‘irregular’ nature

of the highly structured inner parts of NGC 1275, a result of dust, star formation and other features. To remove these we first subtract out all asymmetric parts from NGC 1275 and then fit isophotes to the ‘symmetric’ residual image. We then subtract out these fitted isophotes from the original image. Aperture photometry, with a $1.2''$ aperture, is then performed on the clusters in this subtracted image.

3.2.1. Inner Regions

The inner star clusters whose colors we measure are labeled on Figure 9, and listed in Table 2. The majority of these clusters have similar colors, with $(B-R)_0 \sim 0.3 - 0.7$, with a few blue clusters with $(B-R)_0 \sim 0.0$. This is similar to the broad distribution found by Carlson et al. (1998) for the bright, blue clusters.⁴ Photometry of the inner clusters is also presented in Holtzman et al. (1992), Richer et al. (1993), Norgaard-Nielsen et al. (1993) and Brodie et al. (1998). A comparison to these studies can be effectively done using Table 2 of Brodie et al. (1998). The rough corresponding objects in our Table 2, in comparison to those of Brodie et al. (1998: Table 2), are objects 1, 2, 3, 4, 5, 6 with H2, H3, H4+9, H1, H6, and H5. The average absolute differences between our photometry and the HST photometry of Brodie et al. (1998), using the same Galactic extinction corrections, is ~ 0.24 mag in the B and R bands with $\sigma_{B,R} = 0.28$ and 0.26. The average color difference is $(B-R)_{\text{Brodie}} - (B-R)_{\text{ThisPaper}} \sim 0.20$. Given the slightly different filter systems and approaches used to measuring photometry, we a priori would not expect to measure exactly the same values. The values are, however, consistent within the quoted errors of each measurement. The blue colors match those expected for rather young, aged < 500 Myr, clusters, and the implications of a rather homogeneous population of young clusters will be discussed in §4.2.

3.2.2. Outer Stellar Regions

The pioneering U-band images taken by MOS96 detected extended blue regions in NGC 1275 that are not associated with the ionized filaments. We also detect new outer star clusters, shown in Figure 8 and labeled as clusters 17 - 22 in Table 2, that are roughly $1'$ from the center of NGC 1275. These features clearly extend beyond the main stellar body of NGC 1275 as seen in Figure 1 and in the B–R color map (Figure 8). We measure very blue colors with $(B-R)_0 \sim -0.3$ to 0.0 (Table 2), consistent with an age of < 100 Myr, younger than the inner clusters. However, differential reddening may also be partially responsible for these color differences, thus we can not rule out the possibility that they are coeval systems.

The distinction of these clusters from the ionized filaments is demonstrated by comparing Figures 2 and 8, where the $H\alpha + [NII]$ emission and blue continuum are shown. The two main regions of extended star formation have approximate mirror symmetry around the center of NGC 1275, consistent with an origin from either tidal arms/streamers from a galaxy merger, or effects of a bi-polar jet from the nucleus. The loop or ‘arm’ structure in the southeastern region “A” favors the jet model, where stars could be produced around an expanding cocoon driven by a relativistic plasma (see §4.2). The northwestern blue region “B” has a linear structure that could also result from either process.

Region “A” in Figure 8 has a projected linear extent of $\approx 8h_{100}^{-1}$ kpc and region “B” has a projected size of $\approx 15h_{100}^{-1}$ kpc. These features are as narrow as 0.5 kpc in some places and are often sharply defined. Such crisp structures cannot last very long in the absence of additional support, such as magnetic

⁴Carlson et al. also detected a population of faint red clusters that we do not consider here.

fields. For a typical projected distance of $15\text{-}20h_{100}^{-1}$ kpc for the outer parts of these features, the orbital period will be ~ 0.5 Gyr, which sets an upper limit to their lifetimes.

The separation of these zones from the current locations of the bright radio lobes and ionized filaments (MOS96) also suggests that if causally connected the relativistic outflow in NGC 1275 has undergone multiple changes in direction in the last orbital period, or the filaments formed by some other process. We also note the presence of a redder, fainter, and more diffuse plume or arrow (Figure 8), extending from the nucleus to the south-southwest. This might be an example of a somewhat older jet-induced star forming region, or a remnant of the stellar disk of an accreted galaxy.

3.3. The High Velocity System

The HV (8200 km s^{-1}) emission line system can potentially be explained by the superposition of a highly distorted foreground late-type galaxy. This hypothesis has gained acceptance from observational evidence, including the localized position of the HV lines at the northwest corner of NGC 1275 (Rubin et al. 1977, Caulet et al. 1992), HI and X-ray absorption against the radio source indicating that the HV system is in the foreground (DeYoung et al. 1973; Fabian et al. 2000), possible rotation of the HV system (Rubin et al. 1977, Boroson 1990), optical dust lanes and absorption consistent with a late-type galaxy (Keel 1983; Keel & White 2001), an optical spectrum consistent with late-type HII regions without shocks (Kent & Sargent 1979), and a spectrum with ordinary stellar Ca II triplet absorption at $\lambda 8498$ and Na I D lines (Boroson 1990) at the same velocity as the HV system. We also observe that the star clusters projected towards the HV system have blue colors with $(B-R)_0 \sim 0.1 - 0.4$, possibly indicating an age slightly younger than the clusters associated with the inner LV system clusters (Table 2 & Figure 9). There are however very blue clusters in the outer parts of NGC 1275 that are not in the projected location of the HV system (§3.2.1; Figure 8).

What is not generally agreed upon is the role this HV system is playing in the evolution of NGC 1275. The distance of the HV material from the center of NGC 1275 is an important parameter for understanding this problem. A significant amount of non-thermal emission is coming from NGC 1275 at the location of the HV system (Pedlar et al. 1990), and a spatial correspondence may exist between the HV and LV emission systems where the HV gas is present (Unger et al. 1990, Caulet et al. 1992). $H\alpha$ gas with velocities between the HV and LV system also exists (Ferruit et al. 1997), suggesting a possible connection. These observations allow for the possibility that some interaction is occurring between the HV system and the main NGC 1275 system (see Boroson 1990 and references therein; Fabian et al. 2000), and led Pedlar et al. (1999) to conclude that the HV system is probably infalling and within 30 kpc of the NGC 1275 nucleus.

While an infalling galaxy is an attractive model for the HV system, it has not yet been established how it would fully describe the many peculiarities of the HV material. The ionized gas properties of the HV system suggest that it could be a moderate-size, late-type field galaxy (Unger et al. 1990). However, the estimated rotational velocity of 300 km s^{-1} would be high for such an object. Others have also argued that the HI gas content is too low (van Gorkom & Ekers 1983) for a late-type galaxy, although gas depletion would be expected for an infalling galaxy only ~ 30 kpc from the cluster core. The structure of the original HV object is likely further obscured by perturbations produced by the environment near NGC 1275.

Other distorted galaxies exist near NGC 1275 (Conselice & Gallagher 1999), demonstrating that this can be a hostile location for smaller galaxies. The large inferred cooling flow in the ICM would imply a higher density ICM (e.g. Fabian et al. 1981; White & Sarazin 1988) offering an efficient mechanism for

removing interstellar gas from an infalling galaxy and thereby further distorting the system. For example, it is possible that a field galaxy interacted with NGC 1275, leaving behind an infalling trail of stripped gas that we see as the HV gas system. Such a feature should be short lived; whether a tidal tail could survive the supersonic passage through the ICM is not obvious, thus models where the gas is strongly bound, such as in a galaxy, perhaps are better candidates for explaining the HV system in a collisional model.

Recently, Dupke & Bregman (2001) discovered X-ray emission to the east and south of NGC 1275 redshifted by several thousand km s^{-1} with respect to the cluster’s central velocity. This material therefore overlaps in velocity with the HV system, but perhaps not spatially. Dupke & Bregman interpret the large peculiar velocities as evidence for an off-center merger in the Perseus cluster by a group or subcluster. However, they do not consider the possibility of a connection to the HV system, whose characteristics also suggest an association with some type of merger process that could be a source of the HV material.

3.4. Motion of the Low Velocity Ionized Gas

The Densepak integral field unit on the WIYN telescope was used to map the LV gas velocity field within NGC 1275 (see §2). Figure 10 shows the outlines of the positions of the fibers on Densepak over the central $30'' \times 40''$ of NGC 1275, while Figure 11 shows the measured velocity distribution. Table 3 lists the positions and velocity values of the gas observed in each fiber.

The velocities across the central $0.33'$ of the ionized gas around NGC 1275 range from 4800 km s^{-1} to 5500 km s^{-1} . A rough velocity gradient can be seen across the area, with higher velocities in the northeast, about $20''$ north of the center of NGC 1275, while there is a minimum velocity near 5000 km s^{-1} in the southwest area⁵. The average velocity in each indicated $10''^2$ region is also indicated. The ionized gas in the inner $30''$ of NGC 1275 could have either a component of rotation about an axis with a position angle of $\sim 120^\circ$, or is involved in a bipolar outflow/inflow. This is similar to the position angle of one of the inner streamers and roughly consistent with rotational flattening responsible for the east-west orientation of the ionized gas complex near the center of NGC 1275. This elongated structure has earlier been recognized as a possible consequence of rotation (e.g. Cowie et al. 1983). Bridges & Irwin (1998) showed that NGC 1275 contains about $10^{10} M_\odot$ of molecular gas in its inner parts, with a similar velocity field and spatial distribution to those of the much smaller mass of ionized gas studied here.

The alignment of both the ionized and molecular inner gas along the major axis of NGC 1275, roughly orthogonal to the direction of the radio jets, the large mass of gas in this region, and its velocity amplitude suggest that this gas is a rotating structure rather than an outflow. The rotation amplitude of 250 km s^{-1} over a radius of $\sim 7 \text{ kpc}$ implies a dynamical mass of $10^{11} M_\odot$. The angular momentum of the inner ionized gas appears to be comparable to that of a typical giant spiral galaxy. While this might result from a cooling flow (e.g. Fabian & Nulsen 1977; Mathews & Bregman 1978) or from a merger with a galaxy, it is not obvious in either case whether or not the gas could align itself along the major axis of NGC 1275 sufficiently rapidly. Whatever the origin of the central gas complex in NGC 1275, it clearly has existed with little or no radial motion for a sufficient time to allow it to orbit NGC 1275 and form a partially relaxed system near the center of the galaxy; the orbital time of $\sim 100 \text{ Myr}$ sets the minimum time scale for this event. Like previous authors, we find a complicated velocity field, suggesting that the inner gas in NGC 1275 is perturbed, possibly by the AGN (Heckman et al. 1989; Bridges & Irwin 1998) or by

⁵This gradient is difficult to see in gray scale versions of this figure.

recent merger(s).

4. Discussion

4.1. Excitation of the Low-Velocity Emission Lines

Emission line intensities from the LV system present as much of a problem as does its spectacular morphology. Optical spectroscopy of NGC 1275 by Kent & Sargent (1979) led them to conclude that the LV filaments could be powered by either photo-ionization from the active BL Lac nucleus, or result from shocked gas. Further analyses by Heckman et al. (1989) and Sabra et al. (2000) also suggest that a combination of shocks and photo-ionization could contribute to making the NGC 1275 filaments, but that neither of these processes alone would suffice.

A key feature is the wide range in filament ionization levels, with pronounced emission from [OI] and [NI] coexisting with [OIII] and [NeIII]. Figure 12 shows an example of our Kitt Peak spectra of the NGC 1275 filaments. Since the ionization levels of H and O are linked by charge exchange reactions, the presence of strong [OI] emission proves that warm neutral gas is present in the filaments. By analogy with conditions in the Crab nebula (Sankrit et al. 1998), we are likely seeing ionized sheaths surrounding neutral filament cores. Thus the density structures of the filaments could play an important role in determining the emitted spectrum, and may be obscuring the ionization mechanisms.

Further complications arise from the short recombination and cooling time scales for the filaments. The recombination time is $\sim 10^5 \text{ yr}/(n_e \text{ cm}^{-3})$ and the cooling time of the ionized gas, if anything, is shorter than this (cf. Osterbrock 1989), so there must be a power source to keep the filaments ionized, or they must be re-formed on comparable time scales. However, the cooling time for the hot ICM near NGC 1275 is $\approx 1 \text{ Gyr}$ (e.g., Fabian et al. 2000; Dupke & Bregman 2001). In the (unlikely) circumstance of no additional heating, the filaments would become neutral much more rapidly than they could be replenished from the ICM. The presence of a spatially coherent system whose extent in light years is larger than their $\sim 10^4 \text{ yr}$ cooling time would be a major puzzle. Evidently the evolution of the filaments is slowed by a source of heat.

How was gas compressed by factors of $>10^3$, to the point where it becomes neutral, in a location where external heating is obviously present? One example of such a process operates in the Crab nebula to create the well-known network of thermal gas filaments (Sankrit et al. 1998) thus the situation is not an impossible one. The ICM around NGC 1275 is the most likely source of gas for the filaments, but then what fills the role of the expanding relativistic plasma in the Crab to cause the ICM in the Perseus cluster to condense into filaments?

Our working hypothesis for filament formation follows the suggestion of MOS96 that the gas filaments around NGC 1275 are produced by an interaction between the ICM and relativistic plasma ejected from the active nucleus of NGC 1275. In this “Crab-like” model, the relativistic plasma has (or had) a higher pressure than the ICM and therefore displaces it. How this occurs depends on the expansion velocity of the relativistic plasma; if it is supersonic relative to the ICM, then we would expect shocks to form at the ICM/plasma interface, but the ICM would be compressed even if the expansion were sub-sonic.

4.1.1. Relativistic Plasma-ICM Interactions

Interactions between jets of relativistic plasma and ambient gas in and around radio galaxies are relatively common; e.g., in Minkowski’s object (van Breugel et al. 1985), Hydra A (McNamara et al. 2000) and Centaurus A (Graham & Price 1981; Morganti et al. 1991; Graham 1998; Mould et al. 2000), where they produce star formation and optical emission line regions. Relativistic plasma ejected from the nuclei of radio galaxies also affects the X-ray emitting thermal gas in several galaxies (e.g. Böhringer et al. 1993; Carilli et. al. 1994; Rizza et al. 2000; McNamara et. al. 2000).

X-ray and radio maps of NGC 1275 (Böhringer 1993, Pedlar et al. 1990, MOS96, Fabian et al. 2000) indicate this type of event may have occurred around NGC 1275. These maps reveal that the radio plasma seems to have displaced the X-ray emitting gas around the northern and southern bases of the filament system. The linear extension of filaments to the north aligns with faint emission seen at low frequencies, possibly the remnants of a former jet structure (Blundell, Kassim, & Perley 2000). The $H\alpha$ emission largely avoids both the current radio lobes and the surrounding X-ray bright areas, but often are exterior to these regions, as expected if they form in displaced gas.

A simple model for this type of interaction is that a near spherical bubble of relativistic gas expands from the galaxy into its surroundings. This bubble or “cocoon” is powered by a jet from the active galactic nucleus (Pedlar et al. 1990; Heinz et al. 1998). The kinetic energy input to the relativistic plasma is estimated to currently be about 10^{43} erg s^{-1} in NGC 1275 (Pedlar et al. 1990), similar to the energy released from the cooling ICM gas. It is therefore energetically possible for the relativistic plasma to influence the ICM. The size of the cocoon at the time it detaches from the jet can be estimated, following Churazov et al. (2000), to be about 50 kpc in NGC 1275.

Possibly a cocoon displaced the hot ICM surrounding the center of NGC 1275 (Böhringer 1993, MOS96). In principle an expanding cocoon could produce large scale shocks, a key aspect of the Heinz et al. (1998) model. Recent observations with *Chandra* of NGC 1275 reveal neither evidence for strong shocks between the radio lobes and the ICM, nor indications that the radio lobes are expanding supersonically (Fabian et al. 2000). From these data and the results of Sabra et al. (2000) it seems unlikely that shocks are currently the major factor in the filament system. However, shocks could have occurred in the past if we are witnessing a late phase of the interaction between the radio lobes and the ICM, after the main expansion stage, as in the evolutionary models of NGC 1275 presented by Reynolds, Heinz, & Begelman (2001).

Clearly the production of filaments involves complex physical processes, and more so if, as is likely, magnetic fields are a significant factor. However, once cool material is produced, it will be much denser than its surroundings. This material is likely to be subject to Rayleigh-Taylor and Kelvin-Helmholtz instabilities, which will act to further concentrate the cooling gas (e.g., Böhringer & Morfill 1998). The combination of large scale gas compression from supersonically expanding radio lobes and subsequent instabilities can plausibly lead to the spectacular NGC 1275 filament system as suggested by MOS96.

While the conceptual model of a radio lobe-ICM interaction producing filaments is attractive, some important issues are unresolved. Most critical is whether the hot ICM can be sufficiently compressed along the boundary of a cocoon so as to cool rapidly enough to create the ionized filaments. For an intrinsic ICM cooling time near the main body of NGC 1275 of <1 Gyr (Fabian et al. 2000), we require compression factors of ~ 10 for the gas cooling time to be shorter than the dynamical time scales of ≈ 100 Myr (see §3.1.1). A strong adiabatic shock produces a factor of 4 increase in density. Thus, with even modest

post-shock cooling, the compressed gas will be able to drop to temperatures of $\leq 10^6$ K during the required time interval. At this point the cooling rate greatly increases due atomic line emission, and the thermal time scales decrease by at least a factor of 10. In addition, the expanding relativistic gas could uplift cool, dense material from the inner parts of the system, as suggested by Churazov et al. (2000), and thereby provide another source of dense material for making filaments.

In this model the filaments come from the ICM, thus it can be tested by comparing the chemical abundances of species in the filaments and the ICM. If this model were accurate the two abundance measurements would be similar. Based on the Perseus cluster ICM chemical abundances measured by Dupke & Arnaud (2001), we would expect the filaments to contain gas with about half of the solar oxygen abundance. Another test can be made by estimating pressures within the filaments. If they form from instabilities in the ICM and are long-lived, then they will be in approximate pressure equilibrium with their surroundings. As we saw in §3.1.1, if the electron densities are as high as the allowed upper limits of $n_e \approx 100 \text{ cm}^{-3}$ given by the [SII] doublet emission line ratios, then the pressures could be roughly equal between the filaments and ICM. We conclude that current observations neither eliminate this model, nor suffice to fully establish its veracity.

4.2. Recent Galaxy Accretion in the NGC 1275 System

4.2.1. The LV System

While NGC 1275 has neither the colors nor the spectrum of a classical elliptical galaxy (e.g. van den Bergh 1977; Wirth et al. 1983; Romanishin 1987), it does have an $R^{1/4}$ radial surface brightness profile, typical of giant ellipticals, in its inner regions (e.g., Schombert 1986; Prestwich et al. 1997). However, an $r^{1/4}$ profile can form on short time scales during mergers between disk galaxies, and is often found in recent mergers, such as Arp 220 and NGC 7252 (Schweizer 1998). Therefore this feature alone does not tell us if NGC 1275 is fundamentally an ancient elliptical galaxy.

Holtzman et al. (1992) presented convincing evidence, from images taken with the Wide Field Planetary Camera 2 (WFPC2) on the *Hubble Space Telescope*, that NGC 1275 contains complicated internal stellar structures. They found what appears to be a spiral arm, or a diffuse asymmetric light feature, near the center of NGC 1275, as well as two ripple patterns to the southeast of the center of the galaxy. We detect in our data two new ripple features (or rings), for a total of four (see Figure 8). We further identify two diffuse “arms” (Figure 8 & 9), one more than Holtzman et al. (1992), with an additional third small “arm” in between. These “arm” features have a surface brightness $\mu_B \sim 22 \text{ mag arcsec}^{-2}$, with moderately blue colors, $(B-R)_0 \sim 0.30$, suggesting that the stars in the ‘arms’ are the same age as the clusters. The magnitude of each arm is about $B = 20.6$, or $M_B \sim -14$. These ‘arms’ could have formed from gas imported from the accreted galaxy, while the ripple features are potentially from the old stellar component. The luminosities of the arms suggests that the accreted object could be either a dwarf galaxy, or disrupted young luminous star clusters.

The small scale features in the main body of NGC 1275 support the idea that this galaxy experienced a merger with a galaxy that contained a non-negligible stellar mass, but likely with a significantly lower mass than NGC 1275 (cf. Schweizer & Seitzer 1988).

Carlson et al. (1989) describe a large population of blue, $B-R \approx 0.3$, star clusters with ages ~ 300 Myr. There is very little spread in the colors of these bright star clusters, hence they could have all been

created at nearly the same time, although uncertainties in internal extinction and background subtraction make precise age-dating of the star clusters difficult (Holtzman et al. 1992; Carlson et al. 1989). Corrected for Galactic extinction, but uncorrected for internal extinction or background light, we find that most star clusters in this region have $(B-R)_0 \sim 0.3 - 0.7$, and absolute magnitudes $M_B \sim -12$ to -15 , corresponding to ages of <1 Gyr for metallicities of >0.1 solar (Kurth et al. 1999). Based on these ages, it seems likely that the most recently completed merger in NGC 1275 took place about 300 Myr ago.

We find further support for this merger being either a recent minor or old major one, in a relative sense, by the use of a color-asymmetry diagram (CAD). The CAD is a diagnostic tool for determining physical properties of galaxies based on the quantitative parameters of asymmetry and color (see Conselice 1997 and Conselice et al. 2000a). Briefly, this approach takes advantage of the natural correlation between mean color and degree of organization in normal galaxies that is broken when a galaxy is disturbed by interactions, which produce higher levels of disorganization than in a normal galaxy of the same color. The organization of the galaxy is measured in terms of an asymmetry parameter (Conselice et al. 2000a).

Among other properties, many nearby galaxies that do not fit on or near the CAD normal galaxy fiducial sequence (dashed line in Figure 13) are undergoing an interaction or recent merger (Conselice et al. 2000a,b). NGC 1275, within a radius that excludes the HV system, has an asymmetry value of $A = 0.16 \pm 0.01$. Asymmetries are computed by rotating an image by 180° , subtracting the rotated image from the original, and then by taking the ratio of the absolute value of the sum of these residuals to the total flux of the galaxy. NGC 1275 has a color $(B - V)_0 = 0.72 \pm 0.03$, corrected for internal and galactic extinction (de Vaucouleurs et al. 1991). These asymmetry and color values do not put NGC 1275 in the area of major mergers (Figure 13, Conselice et al. 2000b), but its asymmetry is somewhat large for what is clearly an underlying spheroidal galaxy, indicating the presence of the faint peculiar rings representing a small perturbation in the mainly symmetric galaxy. The other galaxies in Figure 13 have asymmetries measured at larger radii, where mixing times are longer, than where we measure NGC 1275's value. NGC 1275 is thus even more asymmetric, in a relative sense, than that implied by examining its position on Figure 13.

The broad range of estimated clusters ages around NGC 1275 (Richer et al. 1993; Kaisler et al. 1996) possibly requires an extended star formation history that might not be associated with recent mergers. In the future wide-field high resolution images and integral field spectroscopy of NGC 1275 will allow closer examination of this formation process through a determination of its star cluster formation history.

4.2.2. The HV System

In Figure 8, we note the area of the HV foreground ‘galaxy’ in our color image of NGC 1275. This appears as extra blue light in the northwest quadrant of NGC 1275, where MOS96 also noted a possible coincidence of blue light with the HV emission line system. While we cannot rule out the possibility that some of the excess light in the northwest quadrant is from star formation in the LV system, its location suggests a possible connection with the HV system.

This asymmetric components in this area appears bluer than the rest of NGC 1275 (MOS96) as is readily seen in the B–R color map. If this is the possible HV foreground galaxy, then it contains several thick dust lanes (Keel 1983; Keel & White 2001) and star clusters. These clusters are not present in the $H\alpha$ image of the LV emission from NGC 1275, although some of these clusters are at the LV system redshift of $\sim 5200 \text{ km s}^{-1}$ (Carlson et al. 1998; Brodie et al. 1998). Confirmation of which star clusters are in the HV

system will require further spectroscopy for radial velocity measurements.

The non-detection in the LV H α and the spatial coincidence with the HV system lends credibility to the possibility that some of the star clusters and the underlying starlight could be the remains of the galaxy responsible for the HV emission. The blue light that could be part of the HV system does not resemble any normal galaxy. The star-forming knots are aligned parallel to dust lane features (Figure 8), suggestive of the pattern seen in the arms of spiral galaxies, while the distorted shape of the overall system suggests that dynamical disruption has occurred. Keel and White (2001) further suggest that the highly correlated spatial positions of the dust lanes near the HV system and clusters are strong evidence for an association. In any case, whether LV or HV, these star clusters have essentially the same colors as the spectroscopically confirmed (Brodie et al. 1998) LV clusters (Table 2). Interpreted as similar ages, this would imply a coincidence in the epoch of cluster formation. This could arise as a result of an interaction between the gaseous components of the LV and HV systems, perhaps indicated by the presence of H α gas at velocities bridging those of the two systems (Ferruit et al. 1997).

Cluster formation in a burst of star formation associated with the infall process is also plausible. It would be useful to seek older, redder clusters with high radial velocities as a means to identify an underlying old HV system stellar population that would be an unambiguous signature of a galactic source for the HV stars, versus for example, star formation stimulated by a jet.

The interaction of a late-type field spiral falling towards NGC 1275 would be further complicated by the effects of gas stripping mechanisms. In addition to the usual ram pressure and other gas removal mechanisms associated with a rapid passage through the ICM (whose density would be boosted by the cooling flow), an infalling galaxy also could interact with the expanding relativistic plasma from the AGN in NGC 1275 (Churazov et al. 2000). These stripping processes also offer an explanation for the depleted level of HI gas in the HV system found by van Gorkom and Ekers (1983). If some of the gas forms stars during the interaction/stripping, which must be associated with shocks given the clearly supersonic relative velocities, then the HV stellar populations produced would have unusual spatial distributions and should be no older than the time since the infalling galaxy entered the cluster.

In summary, our observations allow a model where the HV system towards NGC 1275 was produced by an infalling galaxy. Identification of pre-infall HV stellar populations or star clusters with ages of $>$ few Gyr would be consistent with this hypothesis. Until then the possibility remains that the HV system formed by a more exotic process, such as an interaction between a jet from the AGN and something else (galaxy, gas cloud) in the vicinity of NGC 1275. However, an additional hint that the HV system might be part of a single event comes from the high redshift X-ray emission component in the Perseus cluster found by Dupke & Bregman (2001).

5. Summary and Discussion

In this paper we present new observations of the bizarre NGC 1275 system in the Perseus cluster of galaxies. High quality WIYN Telescope images of the LV system of ionized gas filaments allow important structural distinctions to be made. We show that filaments have roughly constant surface brightness along their lengths, inconsistent with photoionization directly from the AGN (see also Heckman et al. 1989; Sabra et al. 2000). Tangential filaments generally curve around the central galaxy, suggesting gas compression by an outflow from NGC 1275 rather than cooling in a pure inflow. Filaments also show rich structures, including bright knots, to the limits of our angular resolution ($\sim 150h_{100}^{-1}$ pc).

We follow the suggestion of MOS96 in interpreting the tangential filaments as regions where the expanding relativistic plasma from the AGN in NGC 1275 displaced and compressed the ICM, which then rapidly cooled (Böhringer et al. 1993; Heinz et al. 1998; Churazov et al. 2000; Fabian et al. 2000). Gas along the boundaries of the radio lobes may be further concentrated by Kelvin-Helmholtz instabilities and radial filaments can form from the actions of additional cooling and Rayleigh-Taylor instabilities. The resulting filaments are expected to consist of tubes or ribbons, likely with complex substructure and small ionized gas filling factors. If this picture is correct, then we expect the gas in the filaments to have the same abundances as the ICM from which they formed, and to be in approximate pressure equilibrium with their surroundings. Abundances, excitation and ionization states for tangential and radial filaments should also be similar to one another at a given distance from the center of NGC 1275. Problems remain with this model, for example it does not suggest how long the filaments should last. The lifetime would depend on how stable the radio output is, where the ionization comes from, magnetic fields, etc., all things we do not completely understand yet. Future measurements of the internal velocities of individual components of the filaments will provide useful insights into these problems. For near pressure equilibrium models, internal speeds will be roughly sonic, while bulk motions can be much faster, albeit still sub-sonic with respect to the medium in which the moving filaments are embedded.

The source of filament ionization is not completely understood, but is unlikely to be a simple result of either shocks or photoionization (cf., Sabra et al. 2000). However, any heating process cannot be too effective since the [OI] and [NI] emission indicate the presence of neutral gas within the filaments. It is therefore possible that the filaments hide a significant gas mass within their neutral cores. However, we find only a few examples of blue stars associated with ionized filaments, thus they generally are not so dense as to support extensive star formation.

Our data agree with the MOS96 finding that in the past, dense filaments probably were sites of star formation outside of the main body of NGC 1275. Two regions containing young blue star clusters extend over ~ 5 kpc on either side of the main body of NGC 1275. The existence of star formation in gas compressed by the relativistic plasma of a radio source would not be unique to NGC 1275, but we do not yet properly understand this process. It is not obvious why extensive star formation occurred in some regions in the relatively recent past (<1 Gyr on the basis of B–R colors and dynamical evolution time scale arguments), but not at the present time.

We further demonstrate that morphological properties of the inner portions of NGC 1275’s ripples (or rings; Figure 8) are consistent with a recent minor merger (see Schweizer & Seitzer 1988). From the sizes of these tidal features we estimate that the merger is no older than a few $\times 10^8$ years, the same age as the blue star clusters, and thus a likely cause of the star formation, blue colors and A-type spectrum seen in the central regions of NGC 1275. Rich star clusters are frequently observed in interacting/merging galaxies (e.g., Whitmore 2000). Moreover, gravitational instability can occur within tidal tails (e.g., Duc and Mirabel 1999) perhaps providing an explanation for the spatially extended blue stellar features we identify. If this past event also produced an outburst from the AGN, it could unify the properties of NGC 1275 by creating radio lobes, and therefore ionized filaments.

Using the WIYN integral field spectrograph, we measure the velocity structure of the inner part of the LV ionized gas, finding evidence for rotation in an otherwise chaotic velocity field, where the velocity spread is ≈ 250 km s^{-1} . The velocity field in the inner ionized gas is similar to that of the much larger mass of molecular gas in the same area (Bridges & Irwin 1998). The east-west extension of the inner complex of ionized gas could reflect the influence of rotational flattening, suggesting that this gas reservoir is partially relaxed. It is not clear where the huge amount of cool ISM within NGC 1275 came from. If it is due to the

cooling flow, then a process must exist to align the gas angular momentum vector with the minor axis of the stellar body of NGC 1275 before the gas has settled into a dynamically cool disk. The large amount of dust in this material also requires that extensive star formation took place to pollute what should have been relatively dust-free gas from the ICM. If a significant part of the ISM in NGC 1275 was supplied by mergers, then the merged galaxies must have been extremely gas rich, or were possibly a small group of gas rich systems, that could also produce the large velocity gradient seen in the Perseus cluster X-ray gas by Dupke & Bregman (2001).

The excess stellar surface brightness distribution near the HV ionized is distorted and asymmetric with blue optical colors, as previously discussed by MOS96 and others. The HV system could therefore result from a galaxy interacting with NGC 1275. Star formation in the stripped ISM could be triggered by this interaction, further complicating the structure of this region. Additional radial velocity measurements of the excess blue starlight and a full range of star clusters can provide sharper tests of the infalling galaxy model. If the HV system is associated with the remains of an infalling galaxy that is not yet completely disrupted, then NGC 1275 recently has accreted at least two galaxies – one for the HV system interacting with the ICM of the cluster, and at least one more to make the ripples, rings and star clusters in its main body. This would further suggests that we are seeing the final demise of a small group of galaxies that entered the Perseus cluster. Other galaxies with positions and velocities close to the HV system would be further evidence of this. Hierarchical clustering models of structure formation lead to the formation of clusters of galaxies by the merging of galaxies, so some ongoing accretion/assimilation may be expected.

While tentative explanations exist for several aspects of NGC 1275, others remain as mysteries. It is not clear why the core of the Perseus cluster should host strong interactions at the present epoch, especially since the remainder of the cluster is remarkably free from low velocity galaxy interactions and starbursting galaxies (Conselice, Gallagher, & Wyse 2001). Another problem is the presence of apparently linear dust lanes (Figures 1, 2 & 8), including large clumps of dust near the HV system not seen in other areas. If the HV system’s gas and stars are being distorted by an interaction with the ICM and expanding energetic radio plasma, then how does the dust survive? Furthermore, neither the role, nor the extent of the cooling flow in Perseus is fully understood. This leads to unresolved questions as to how the cooling flow affects the various components of the cluster, particularly its inner parts in the critical region around NGC 1275 (e.g., Fabian et al. 2000).

Further observations of the Perseus cluster with X-ray satellites such as *Chandra* and XMM to obtain higher resolution imaging and detailed abundance measurements of the ICM from X-ray spectroscopy should clarify this and several other issues. Additional studies at other wavelengths are needed, including efforts to better define the characteristics of the young clusters, especially their ages and kinematics, as well as high angular resolution observations designed to explore the internal structures of the H α filaments. Gaining a proper description of what is happening in and around NGC 1275 remains an important milestone for understanding the evolution of central galaxies in rich clusters.

We thank the “WIYN Crew” for providing a superb and smoothly operating observatory, and Birgit Otte for assistance on several technical aspects of this research. Annette Ferguson kindly provided the opportunity for us to take long-slit spectra during a run at the KPNO 4m. We also thank Lisa Frattare for creating the color image of the ionized gas around NGC 1275 with our WIYN images (Figure 1), and John Hoessel and an anonymous referee for useful comments. This work was supported in part by the National Science Foundation through grants AST-9803018 to the University of Wisconsin and AST-9804706 to the Johns Hopkins University (RFGW). JSG appreciates support provided by the Vilas Trustees through the University of Wisconsin Graduate School. CJC also gratefully acknowledges support from the

Wisconsin/NASA Space Grant Consortium, a Grant-in-aid of research award from the Benjamin A. Gould fund from Sigma-Xi and the National Academy of Sciences and a Graduate Student Research Program (GSRP) Fellowship from NASA.

REFERENCES

- Barden, S.C., & Wade, R.A. 1988, in “Fiber Optics in Astronomy”, p.113 (ASP Press: San Francisco, CA)
- Böhringer, H., & Morfill, G.E. 1998, *ApJ*, 330, 609
- Böhringer, H., Voges, W., Fabian, A.C., Edge, A.C., & Neumann, D.M. 1993, *MNRAS*, 264, 25L
- Boroson, T.A. 1990, *ApJ*, 360, 465
- Bridges, T.J., & Irwin, J.A. 1998, *MNRAS*, 300, 967
- Brodie, J. Schroder, L.L., Huchra, J.P., Phillips, A.C., Kissler-Patig, M., & Forbes, D.A. 1998, *AJ*, 116, 691
- Burbidge, E.M. & Burbidge, G.R. 1965, *ApJ*, 142, 1351
- Burstein, D., & Heiles, C. 1984, *ApJS*, 54, 33
- Cardelli, J.A., Clayton, G.C., & Mathis, J.S. 1989, *ApJ*, 345, 245
- Carilli, C.L., Perley, R.A., & Harris, D.E. 1994, *MNRAS*, 270, 173
- Carlson, M.N., et al. 1998, *AJ*, 115, 1778
- Caulet, A., et al. 1992, *ApJ*, 388, 301
- Churazov, E., Forman, W., Jones, C., & Böhringer, H. 2000, *A&A*, 356, 788
- Cowie, L.L., Fabian, A.C., & Nulsen, P.E.J. 1980, *MNRAS*, 191,399
- Cowie, L.L, Hu, E.M., Jenkins, E.B., & York, D.G. 1983, *ApJ*, 272, 29
- Conselice, C.J. 1997, *PASP*, 107, 1251
- Conselice, C.J., & Gallagher, J.S. 1999, *AJ*, 117, 75
- Conselice, C.J., Bershady, M.A., & Jangren, A. 2000a, *ApJ*, 529, 886
- Conselice, C.J., Bershady, M.A., & Gallagher, J.S. 2000b, *A&A*, 354, 21L
- Conselice, C.J., Gallagher, J.S., & Wyse, R. 2001, in prep.
- De Young, D.S., Roberts, M.S., & Saslaw, W.C. 1973, *ApJ*, 185, 809
- de Vaucouleurs, G., de Vaucouleurs, A., Corwin, H.G., Buta, R., Paturel, G., & Fouquie, P. 1991, Third Reference Catalog of Bright Galaxies (Springer: New York)
- Duc, P. & Mirabel, I. 1999, in ‘Galaxy Interactions at Low and High Redshift’, IAU Symposium 186, eds J. Barnes and D. Sanders, p61
- Dupke, R. A. & Bregman, J. N. 2001, *ApJ*, 547, 705
- Dupke, R. A. & Arnaud, K. A. 2001, *ApJ*, 548, 141
- Dubinski, J. Mihos, J.C., & Hernquist, L. 1999, *ApJ*, 526, 607
- Fabian, A.C., & Nulsen, P.E.J. 1977, *MNRAS*, 180, 479
- Fabian, A.C., Hu, E.M., Cowie, L.L., & Gindlay, J. 1981, *ApJ*, 248, 47
- Fabian, A.C., Nulsen, P.E.J., & Canizares, C.R. 1982, *MNRAS*, 201, 933

- Fabian, A. C., Sanders, J. S., Ettori, S., Taylor, G. B., Allen, S. W., Crawford, C. S., Iwasawa, K., Johnstone, R. M., & Ogle, P. M. 2000, *MNRAS*, 318, L65
- Faber, S.M. 1993, in *ASP Conf. Ser. 48, The Globular Cluster-Galaxy Connection*, ed. G.H. Smith and J.P. Brodie (San Francisco: ASP), 601
- Ferruit, P., Adam, G., Binette, L., & Pecontal, E. 1997, *New Astronomy*, 2, 345
- Graham, J.A., & Price, R.M. 1981, *ApJ*, 247, 813
- Graham, J.A. 1998, *ApJ*, 502, 245
- Grimberg, B.I., Sadler, E.M., & Simkin, S.M. 1999, *ApJ*, 521, 121
- Heckman, T.M. 1981, *ApJ*, 250L, 59
- Heckman, T.M., Baum, S.A., van Breugel, W.J.M., & McCarthy, P. 1989, *ApJ*, 338, 48
- Heinz, S., Reynolds, C.S., & Begelman, M.C. 1998, *ApJ*, 501, 126
- Hester, J.J., et al. 1996, *ApJ*, 456, 225
- Holtzman, J.A., et al. 1992, *AJ*, 103, 691
- Hu, E.M., Cowie, L.I., Kaaret, P., Jenkins, E.B., York, D.G., & Roesler, F.L. 1983, *ApJ*, 275, 27L
- Hubble, E. 1931, *ApJ*, 74, 63
- Huchra, J.P., Vogeley, M.S., & Geller, M.J. 1999, *ApJS*, 121, 287
- Humason, M.L. 1932, *PASP*, 44, 267
- Kaisler, D., Harris, W.E., Crabtree, D.R., & Richer, H.B. 1996, *AJ*, 111, 2224
- Keel, W.C. 1983, *AJ*, 88, 1579
- Keel, W.C., & White, R.E., III. 2001, *AJ*, 121, 1442
- Kent, S.M., & Sargent, W.L.W. 1979, *ApJ*, 230, 667
- Koekemoer, A.M., O’Dea, C.P., Sarazin, C.L., McNamara, B.R., Donahue, M., Voit, G.M., Baum, S.A., & Gallimore, J.F. 1999, *ApJ*, 525, 621
- Kurth, O. M., Fritze-v. Alvensleben, U. & Fricke, K. J. 1999, *A&AS*, 138, 19
- Lynds, C.R. 1970, *ApJ*, 159, L151
- Mathews, W.G., & Bregman, J.N. 1978, *ApJ*, 224, 308
- McNamara, B.R., O’Connell, R.W., & Sarazin, C.L. 1996, *AJ*, 91
- McNamara, B.R., Wise, M., Nulsen, P.E.J., David, L.P., Sarazin, C.L., Bautz, M., Markevitch, M., Vikhlinin, A., Forman, W.R., Jones, C., & Harris, D.E. 2000, *ApJ*, 534, 135L
- Minkowski, R. 1955, *Carnegie Yearbook*, 54, 25
- Minkowski, R. 1957, In *IAU Symposium No. 4, Radio Astronomy*, ed. H.C. van de Hulst (Cambridge University Press, Cambridge), p. 107
- Moore, B., Lake, G., & Katz, N. 1998, *ApJ*, 495, 139
- Morganti, R. et al. 1991, *MNRAS*, 249, 91
- Mould, J.R., et al. 2000, *ApJ*, 536, 266
- Norgaard-Nielsen, H.U., Goudfrooij, P., Jorgensen, H.E., & Hansen, L. 1993, *A&A*, 279, 61
- Oke, J.B. 1974, *ApJS*, 27, 21

- Osterbrock, D.E., 1989, “Astrophysics of Gaseous Nebulae and Active Galactic Nuclei”, University Science Books, Mill Valley, California, USA
- Pedlar, A et al. 1990, MNRAS, 246, 477
- Prestwich, A.H., Joy, M., Luginbuhl, C.B., Sulkanen, M., Newberry, M. 1997, ApJ, 477, 144
- Quinn, P.J. 1984, ApJ, 279, 596
- Reynolds, C.S., Heinz, S., & Begelman, M.C. 2001, ApJ, 549, L179
- Richer, H.B., Crabtree, D.R., Fabian, A.C., & Lin, D.N.C. 1993, AJ, 105, 877
- Rizza, E., Loken, C., Bliton, M., Roettiger, K., Burns, J.O., & Owen, F.N. 2000, AJ, 119, 21
- Romanishin, W. 1987, 323, 113L
- Rubin, V.C., Ford, K., Peterson, C.J., & Oort, J.H. 1977, ApJ, 211, 693
- Sabra, B. M., Shields, J. C., & Filippenko, A. V. 2000, ApJ, 545, 157
- Sankrit, R. et al. 1998, ApJ, 504, 344
- Sarazin, C.L., & O’Connell, R.W. 1983, ApJ, 268, 552
- Schombert, J.M. 1986, ApJS, 60, 603
- Schweizer, F. 1980, ApJ, 237, 303
- Schweizer, F., & Seitzer, P. 1988, ApJ, 328, 88
- Schweizer, F. 1998, in Galaxies: Interactions and Induced Star Formation ed. D. Friedli, L. Martinet, & D. Pfenniger (Springer-Verlag: Berlin, Heidelberg), p. 105
- Seyfert, C.K. 1943, ApJ, 97, 28
- Shields, J.C., & Filippenko, A.V. 1990, ApJ, 353, 7L
- Silk, J., Djorgovski, S., Wyse, R. F. G., & Bruzual, A. G. 1986, ApJ, 307, 415
- Struble, M.F., & Rood, H.J. 1991, ApJS, 77, 363
- Unger, S.W., Taylor, K., Pedlar, A., Ghataure, H.S., Penston, M.V., & Robinson, A. 1990, MNRAS, 242, 33
- van Breugel, W., Filippenko, A.V., Heckman, T., & Mikey, G. 1985, ApJ, 293, 83
- van den Bergh, S. 1977, AN, 298, 285
- van Gorkom, J.H., & Ekers, R.D. 1983, 267, 528
- Villar-Martin, M., Tadhunter, C., Morganti, R., Axon, D., & Koekemoer, A. 1999, MNRAS, 307, 24
- White III, R.E., & Sarazin, C.L. 1988, ApJ, 335, 688
- Whitmore, B. 2000, in ‘Dynamics of Galaxies from the Early Universe to the Present’, ASP Conference series vol 197, eds F. Combes, G. Mamon and V. Charmandaris, p315
- Wirth, A., Kenyon, S.J., & Hunter, D.A. 1983, ApJ, 269, 102

TABLE 1
H α EMISSION FLUXES AND INTENSITIES OF PERSEUS FILAMENTS^a

| Number | R(kpc \times h ₁₀₀ ⁻¹) ^b | δ R.A. (") ^b | δ Dec. (") ^b | F (10 ⁻¹⁵ erg s ⁻¹ cm ⁻²) | I (10 ⁻¹⁵ erg s ⁻¹ cm ⁻² arcsec ⁻²) |
|--------|--|--------------------------------|--------------------------------|---|--|
| 1 | 17.6 | -28.0 | -63.2 | 8.4 | 2.7 |
| 2 | 15.6 | -26.0 | -55.4 | 21.2 | 6.8 |
| 3 | 16.2 | -0.2 | -63.8 | 4.1 | 1.3 |
| 4 | 6.7 | -1.4 | -26.4 | 18.9 | 6.0 |
| 5 | 11.5 | -44.6 | 6.8 | 5.6 | 1.8 |
| 6 | 8.5 | -24.4 | 23.2 | 17.8 | 5.7 |
| 7 | 20.2 | -74.4 | 28.2 | 6.6 | 2.1 |
| 8 | 16.5 | -48.0 | 43.4 | 6.3 | 2.0 |
| 9 | 19.8 | -54.2 | 55.6 | 2.8 | 0.9 |
| 10 | 22.6 | -62.4 | 63.0 | 3.7 | 1.2 |
| 11 | 15.8 | -33.8 | 52.2 | 22.5 | 7.2 |
| 12 | 9.0 | -8.2 | 34.4 | 13.4 | 4.3 |
| 13 | 9.1 | 3.4 | 35.6 | 8.1 | 2.6 |
| 14 | 15.9 | 38.4 | -49.2 | 14.2 | 4.5 |
| 15 | 8.3 | 32.2 | -5.6 | 4.0 | 1.3 |
| 16 | 11.0 | 40.0 | 16.4 | 12.2 | 3.9 |
| 17 | 16.3 | 14.2 | 62.4 | 8.9 | 2.8 |
| 18 | 18.1 | 0.0 | 70.8 | 16.7 | 5.3 |
| 19 | 20.7 | -3.8 | 81.4 | 5.2 | 1.7 |
| 20 | 24.4 | -16.6 | 94.4 | 4.6 | 1.5 |
| 21 | 25.5 | 24.8 | 97.0 | 3.7 | 1.2 |
| 22 | 30.4 | -34.8 | 113.8 | 2.1 | 0.7 |
| 23 | 30.3 | -20.4 | 117.0 | 6.8 | 2.2 |
| 24 | 34.0 | -24.8 | 131.0 | 3.7 | 1.2 |
| 25 | 36.8 | -22.2 | 142.4 | 3.1 | 1.0 |
| 26 | 39.5 | -44.0 | 148.4 | 0.9 | 0.3 |
| 27 | 44.0 | -20.8 | 171.2 | 3.8 | 1.2 |
| 28 | 19.7 | -20.0 | 74.6 | 3.7 | ... |
| 29 | 19.2 | -15.6 | 73.6 | 10.8 | ... |
| 30 | 16.1 | 0.0 | 63.0 | 10.6 | ... |
| 31 | 14.5 | 3.4 | 56.8 | 7.0 | ... |
| 32 | 12.6 | -27.6 | 41.0 | 6.9 | ... |
| 33 | 7.7 | 16.0 | 25.6 | 10.7 | ... |
| 34 | 15.8 | -60.8 | -11.8 | 7.2 | ... |
| 35 | 8.3 | -17.4 | -27.6 | 13.2 | ... |
| 36 | 7.8 | 12.0 | -28.2 | 7.3 | ... |
| 37 | 11.5 | 34.0 | -29.6 | 4.2 | ... |
| 38 | 18.2 | 57.8 | -41.6 | 10.5 | ... |

^aEntries 28 through 38 are the H α knots which are labeled as hexagons in Figure 5.

^bColumns 2, 3 and 4 list the distance from the center of NGC 1275, measured in kpc (Column 2) and in differential α (Column 3) and δ (Column 4).

TABLE 2^a
STELLAR FEATURES

| Object | Distance(") | B | R | (B–R) ₀ | B–R _(Brodie) ^b |
|----------------|-------------|--------------------------|--------------------------|--------------------|--------------------------------------|
| 1 | 2.4 | 19.75±0.11 | 19.55±0.11 | 0.20±0.16 | 0.65±0.21 |
| 2 | 3.4 | 19.86±0.14 | 19.20±0.13 | 0.66±0.19 | 0.70±0.21 |
| 3 ^c | 3.5 | 20.02±0.11 | 19.60±0.10 | 0.42±0.15 | 0.65±0.21 |
| 4 | 3.6 | 19.20±0.10 | 18.51±0.10 | 0.69±0.14 | 0.56±0.21 |
| 5 | 4.7 | 20.90±0.20 | 20.50±0.27 | 0.40±0.33 | 0.72±0.21 |
| 6 | 5.4 | 20.51±0.12 | 20.40±0.12 | 0.11±0.17 | 0.42±0.21 |
| 7 | 6.1 | 20.32±0.12 | 20.03±0.12 | 0.29±0.17 | ... |
| 8 | 8.7 | 20.60±0.12 | 20.55±0.13 | 0.05±0.18 | ... |
| 9 | 12.4 | 20.80±0.11 | 20.75±0.12 | 0.05±0.16 | ... |
| 10 | 14.3 | 21.38±0.16 | 20.96±0.17 | 0.42±0.23 | ... |
| 11 | 18.2 | 21.50±0.11 | 21.44±0.14 | 0.06±0.18 | ... |
| 12 | 34.5 | 21.10±0.10 | 20.66±0.10 | 0.44±0.15 | ... |
| 13 | 38.5 | 21.58±0.12 | 21.13±0.10 | 0.45±0.16 | ... |
| 14 | 39.0 | 21.40±0.10 | 21.06±0.11 | 0.34±0.15 | ... |
| 15 | 39.6 | 21.46±0.10 | 21.00±0.10 | 0.46±0.14 | ... |
| 16 | 41.0 | 21.72±0.11 | 21.36±0.10 | 0.36±0.15 | ... |
| 17 | 60.3 | 22.08±0.10 | 22.34±0.12 | -0.26±0.16 | ... |
| 18 | 64.0 | 21.94±0.10 | 22.00±0.11 | -0.06±0.15 | ... |
| 19 | 65.0 | 22.36±0.10 | 22.55±0.13 | -0.19±0.16 | ... |
| 20 | 67.0 | 22.26±0.10 | 22.41±0.12 | -0.15±0.16 | ... |
| 21 | 67.4 | 22.00±0.10 | 22.02±0.11 | -0.02±0.15 | ... |
| 22 | 70.0 | 22.26±0.10 | 21.97±0.10 | 0.29±0.14 | ... |
| A1 | 8.0 | $\mu_B = 21.89 \pm 0.10$ | $\mu_R = 21.53 \pm 0.10$ | 0.36±0.14 | ... |
| A2 | 11.2 | $\mu_B = 21.89 \pm 0.10$ | $\mu_R = 21.66 \pm 0.10$ | 0.23±0.14 | ... |

^aEntries 1 through 16 are for the inner clusters labeled on Figure 9. Entries 17 through 22 are the outer clusters labeled in Figure 8, and entries A1 and A2 are for the ‘arms’ labeled in Figure 9. Entries A1 and A2 list surface brightness instead of magnitudes. These values are corrected for Galactic extinction using $A_B = 0.71$, $A_R = 0.40$.

^bEntries 1 through 6 have B–R colors measured by Brodie et al. (1998), which are listed here.

^cEntry 3 is resolved into two separate clusters, H4 and H9 in the Holtzman et al. (1998) and Brodie et al. (1998) Hubble Space Telescope images. Brodie et al. (1998) also list the parameters of these two clusters as one object.

TABLE 3
DENSEPAK H α VELOCITIES

| R.A. (J2000) | Dec. (J2000) | Velocity (km/s) | R.A. (J2000) | Dec. (J2000) | Velocity (km/s) |
|--------------|--------------|-----------------|--------------|--------------|-----------------|
| 3.330143 | 41.506134 | 5321 | 3.330040 | 41.506134 | 5363 |
| 3.329938 | 41.506134 | 5279 | 3.329835 | 41.506134 | 5242 |
| 3.329732 | 41.506134 | 5295 | 3.330194 | 41.507130 | 5295 |
| 3.330091 | 41.507130 | 5278 | 3.329989 | 41.507130 | 5284 |
| 3.329886 | 41.507130 | 5183 | 3.330040 | 41.508121 | 5197 |
| 3.329938 | 41.508121 | 5076 | 3.329835 | 41.508121 | 5008 |
| 3.330400 | 41.509117 | 5523 | 3.330297 | 41.509117 | 5499 |
| 3.329989 | 41.509117 | 5028 | 3.329886 | 41.509117 | 5068 |
| 3.330348 | 41.510117 | 5491 | 3.329938 | 41.510117 | 5124 |
| 3.329835 | 41.510117 | 5105 | 3.329732 | 41.510117 | 4862 |
| 3.330297 | 41.511108 | 5432 | 3.330194 | 41.511108 | 5418 |
| 3.330091 | 41.511108 | 5428 | 3.329989 | 41.511108 | 5190 |
| 3.329886 | 41.511108 | 5140 | 3.330348 | 41.512100 | 5332 |
| 3.330246 | 41.512100 | 5319 | 3.330143 | 41.512100 | 5258 |
| 3.330040 | 41.512100 | 5275 | 3.329938 | 41.512100 | 5192 |
| 3.329835 | 41.512100 | 5219 | 3.329732 | 41.512100 | 5211 |
| 3.330400 | 41.513100 | 5304 | 3.330297 | 41.513100 | 5377 |
| 3.330194 | 41.513100 | 5261 | 3.330091 | 41.513100 | 5277 |
| 3.329989 | 41.513100 | 5213 | 3.329784 | 41.513100 | 5190 |
| 3.330348 | 41.514099 | 5481 | 3.330246 | 41.514099 | 5473 |
| 3.330143 | 41.514099 | 5292 | 3.330040 | 41.514099 | 5241 |
| 3.329938 | 41.514099 | 5140 | 3.329835 | 41.514099 | 5180 |
| 3.329732 | 41.514099 | 5193 | 3.330194 | 41.515091 | 5512 |
| 3.330091 | 41.515091 | 5330 | 3.329989 | 41.515091 | 5241 |
| 3.329886 | 41.515091 | 5265 | 3.329784 | 41.515091 | 5216 |
| 3.330143 | 41.516087 | 5456 | 3.330040 | 41.516087 | 5430 |
| 3.329938 | 41.516087 | 5377 | 3.329835 | 41.516087 | 5275 |
| 3.329732 | 41.516087 | 5241 | 3.330400 | 41.517082 | 5058 |
| 3.330091 | 41.517082 | 5422 | 3.329989 | 41.517082 | 5423 |
| 3.329886 | 41.517082 | 5347 | 3.329783 | 41.517082 | 5268 |
| 3.330040 | 41.518074 | 5373 | 3.329938 | 41.518074 | 5414 |
| 3.329835 | 41.518074 | 5375 | 3.329732 | 41.518074 | 5306 |

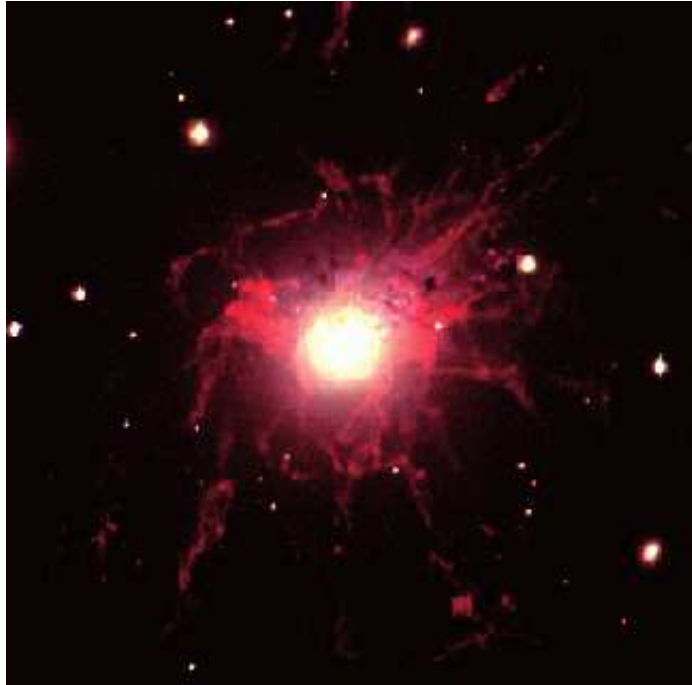


Fig. 1.— Combined color image of NGC 1275 using the B, R, and $H\alpha$ WIYN filters. The ionization structure can clearly be seen, including the tangential filaments oriented in the east-west direction and the longer $50h_{100}^{-1}$ kpc filaments seen projecting towards the north and south. **Note that this figure is best seen in color.**

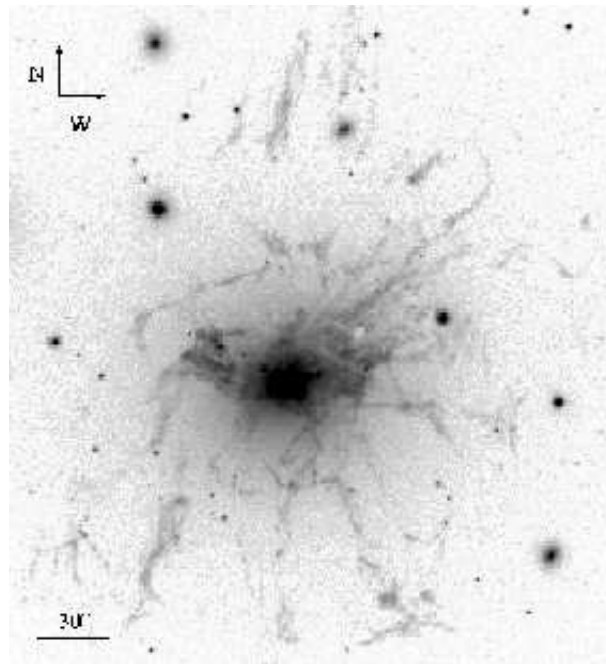


Fig. 2.— An $H\alpha$ image, before continuum subtraction, showing the low-velocity system's ionized gas filaments.

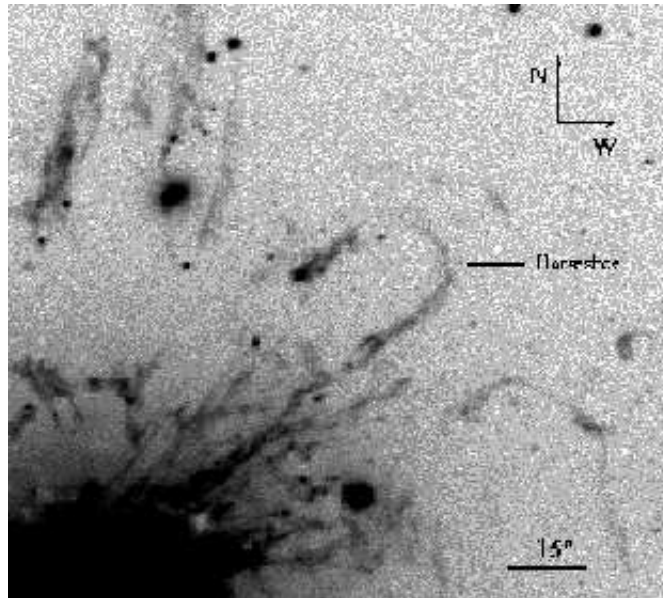


Fig. 3.— Close up of Figure 2 showing an example of a radial filament. This particular filament reverses direction, a possible example of a magnetic Rayleigh-Taylor instability.

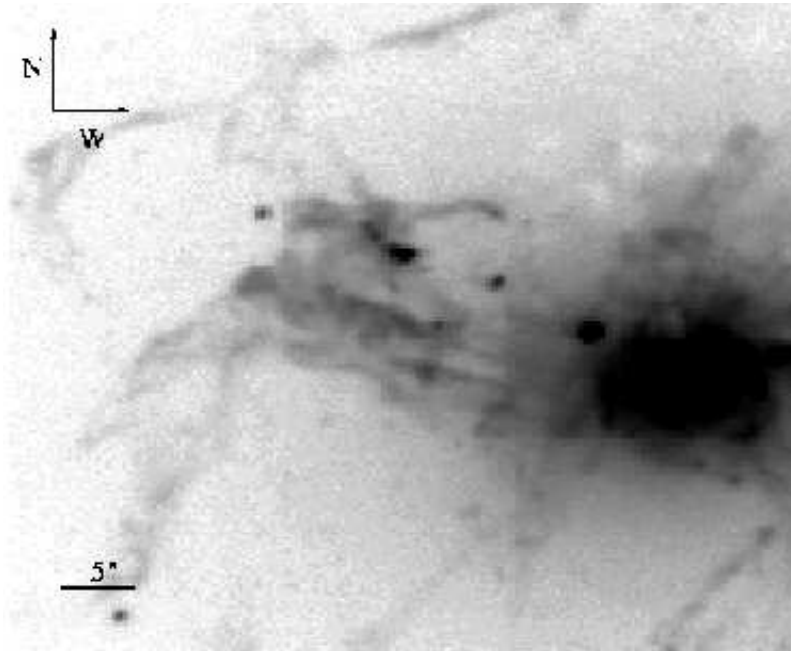


Fig. 4.— Close up of Figure 2 showing examples of tangential filaments that are possibly the instability interface between the radio plasma and the cooling flow X-ray gas.

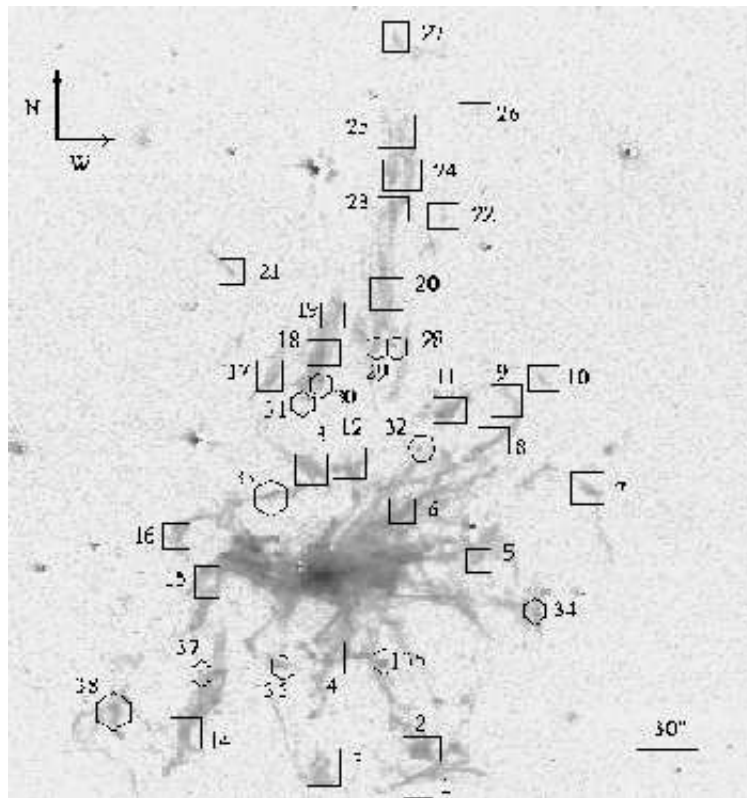


Fig. 5.— Continuum subtracted $H\alpha$ map of NGC 1275 showing the locations of areas used to measure the intensities of emission features listed in Table 1. The hexagons are for $H\alpha$ knots, and boxes are for diffuse areas. **Note:** to properly view this image, please obtain the version of this paper at: <http://www.astro.wisc.edu/~chris/pera.pa>.

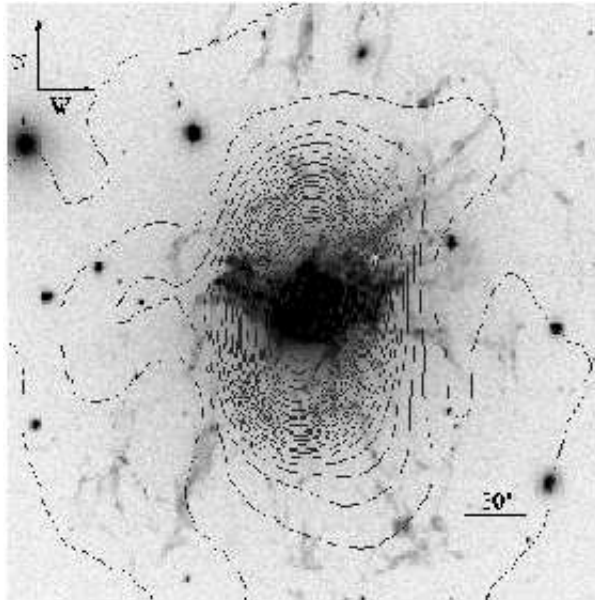


Fig. 6.— $H\alpha$ emission with 1320 MHz radio contours superimposed.

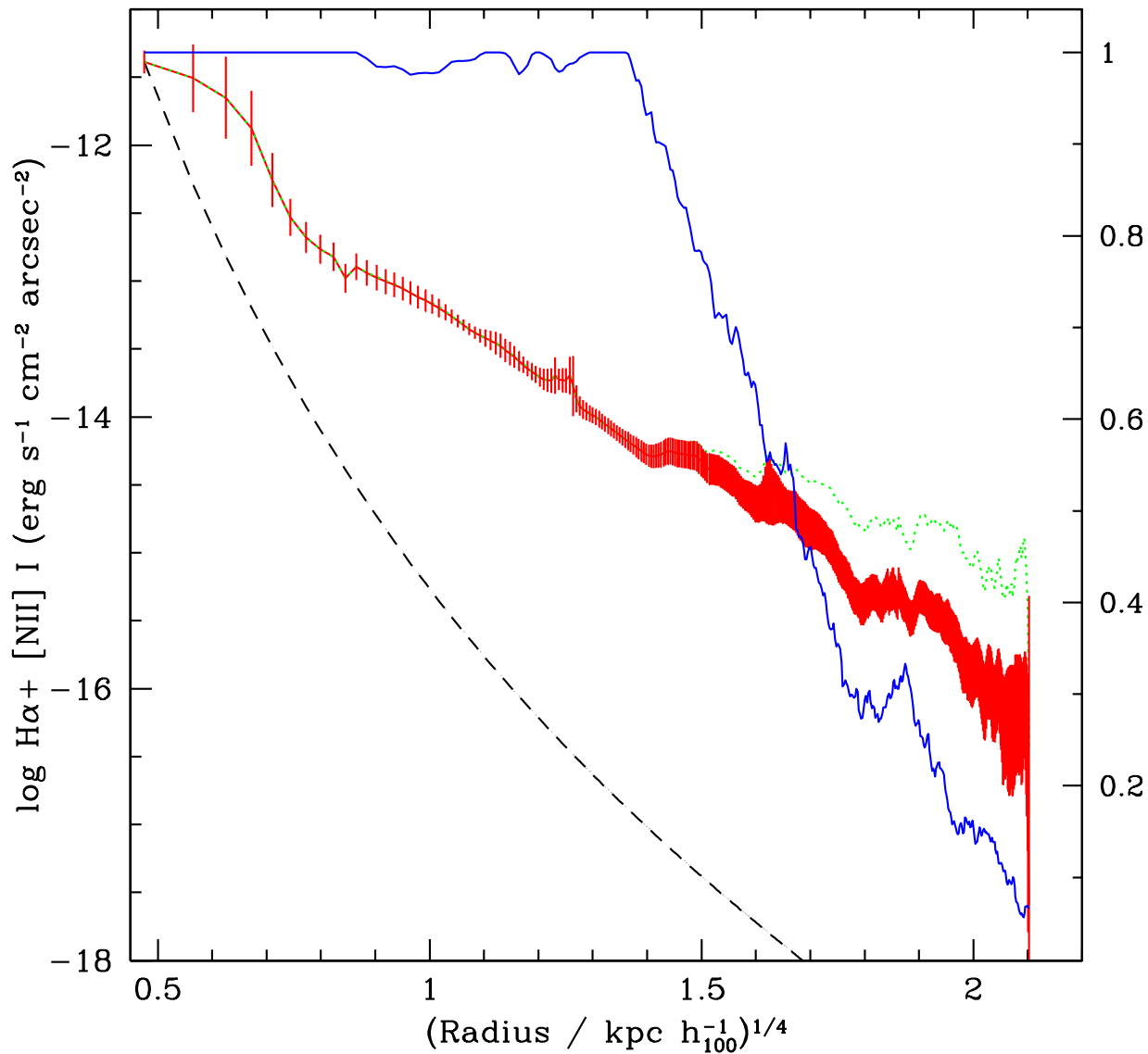


Fig. 7.— The observed mean H α intensity profile of the ionized gas around NGC 1275, as measured in elliptical apertures, is shown as a red line with error bars, plotted on the left intensity scale. The dashed line shows the predicted intensity with projected radius, R , for a central ionization source model with the only losses being r^{-2} dimming. Using the scale on the right, we show the upper limit to the projected ionized gas filling factor versus radius (blue solid line). The inner $3.8h_{100}^{-1}$ kpc is almost completely filled with overlapping filaments, while the outer parts of the system are very sparsely occupied. The green dotted line above the mean intensity profile at larger radii illustrates the brightness that would be observed at each radius if the ionized gas projected filling factor were unity. **Note that this figure is best seen in color.**

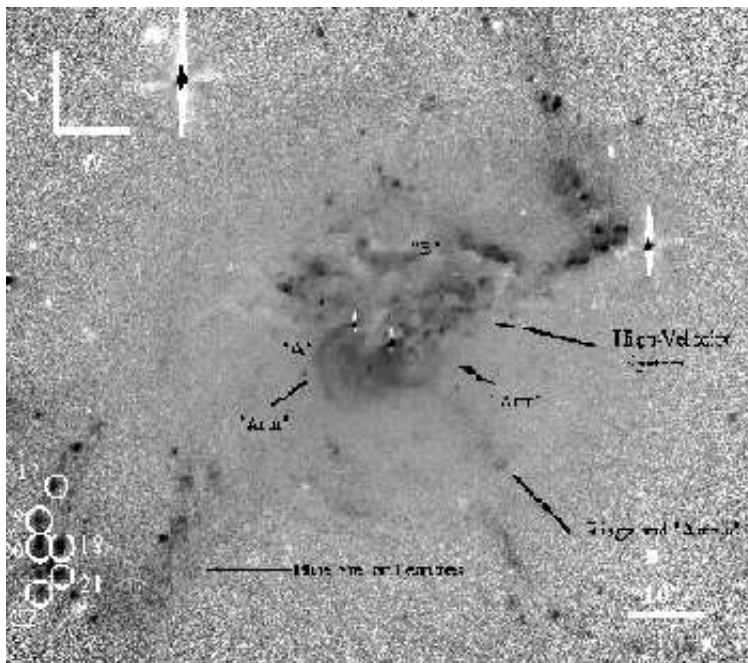


Fig. 8.— (B–R) color image of the central parts of NGC 1275. Darker is bluer. Several features stand out in the image, including the HV system and its associated dust. A blue streak of star clusters can be seen towards the north-west and south-east of the center. South of the center of NGC 1275 are four rings, tidal arms, and an arrow feature, all indications of recent merger activity (see text). The labeled clusters have photometric properties listed in Table 2. **Note: to properly view this image, please obtain the version of this paper at: <http://www.astro.wisc.edu/~chris/pera.pa>.**

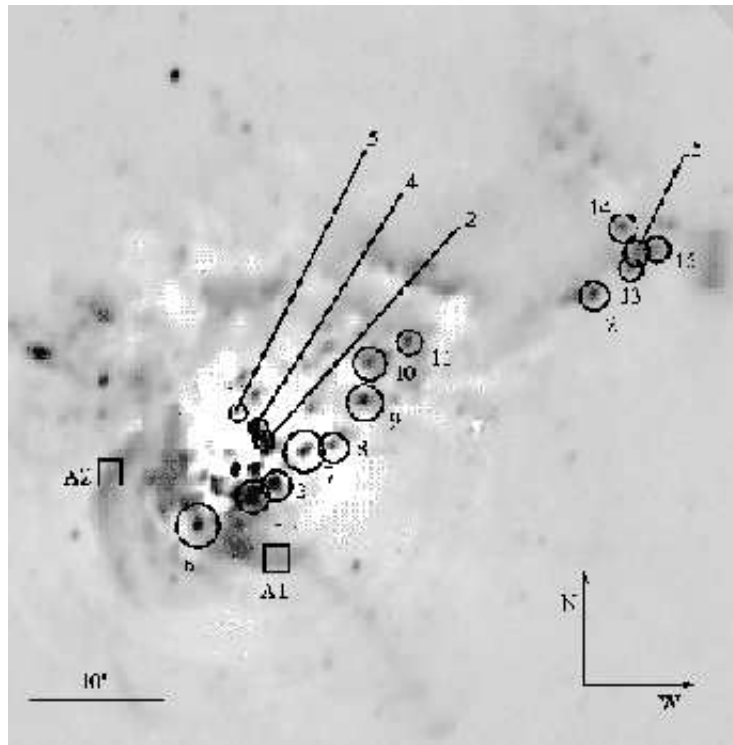


Fig. 9.— Inner stellar features of the NGC 1275 system. Star clusters whose photometry is listed in Table 2 are circled. The areas where features of the ‘arms’ are measured are labeled as boxes and A1, A2. This figure can be compared with Figure 8 by the location of the two ‘arms’. **Note: to properly view this image, please obtain the version of this paper at: <http://www.astro.wisc.edu/~chris/pera.pa>.**

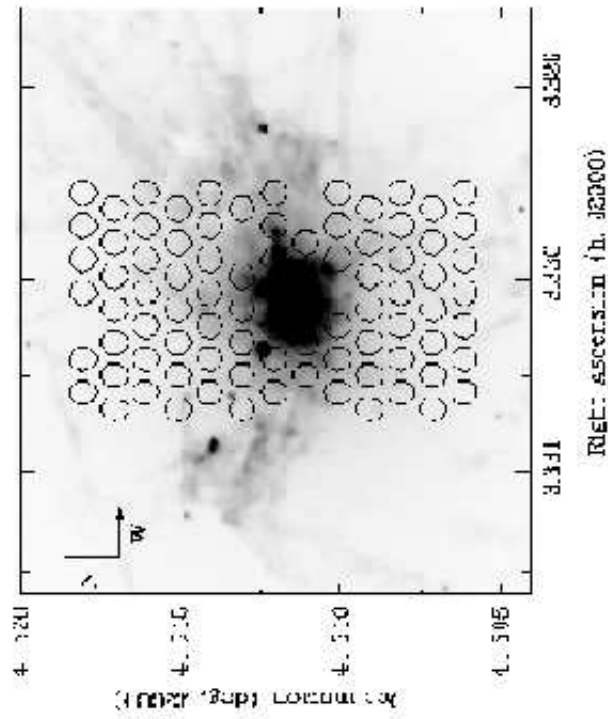


Fig. 10.— Fiber positions of Densepak across the center of NGC 1275.

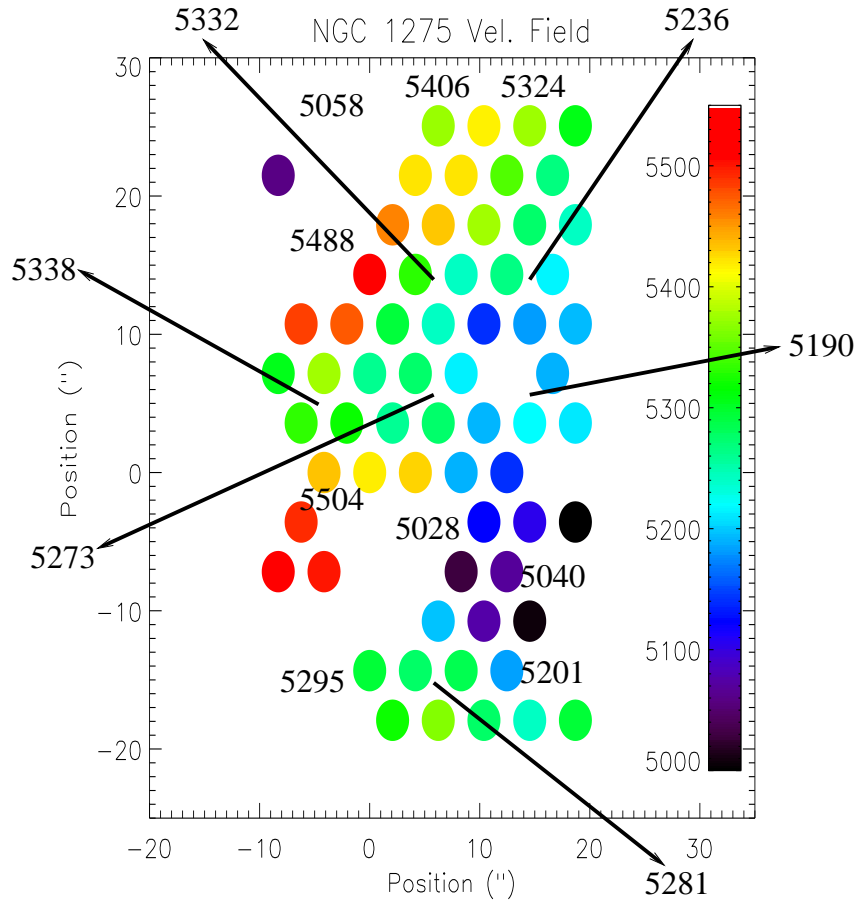


Fig. 11.— Velocity field of the central 45'' of NGC 1275. The velocity range is about 500 km s^{-1} , with an apparent rotation from south-east to north-west at a position angle of 120° . The gradient is clear when imaged is viewed in color, although the gradient can be seen by examining the average velocities for 10'' square boxes which are labeled. **Note that this figure is best seen in color.**

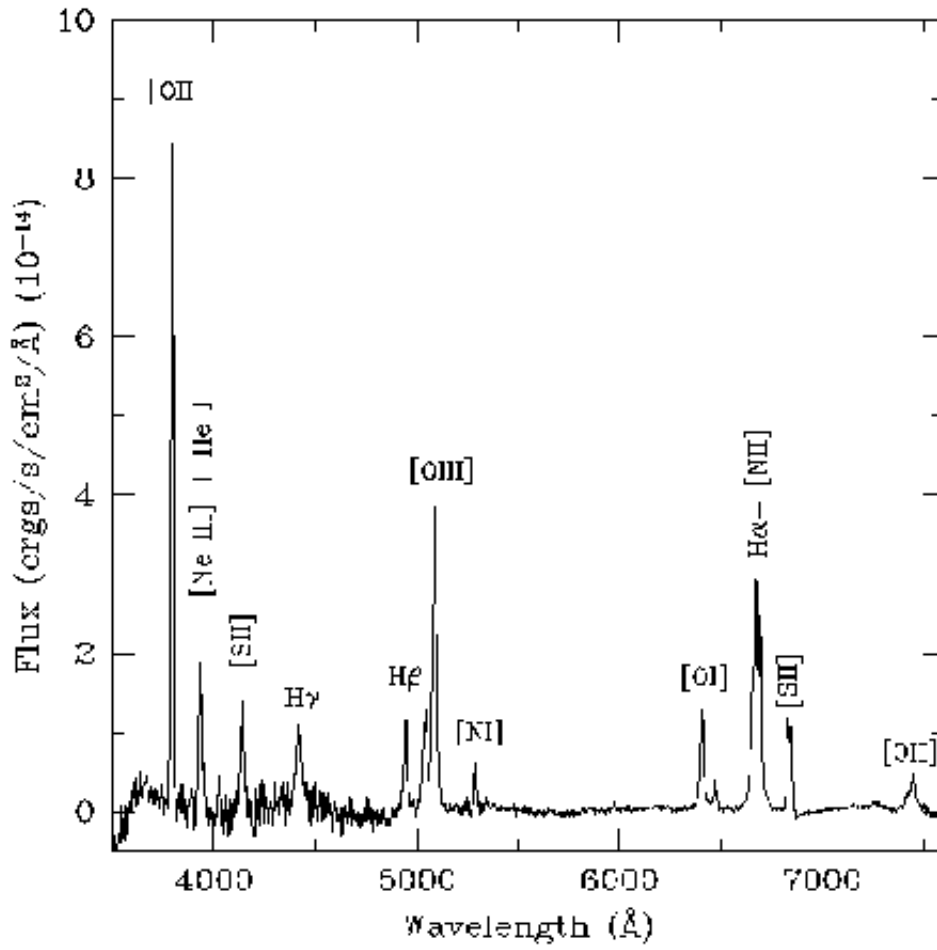


Fig. 12.— Long-slit spectrum of an H α filament near the center of NGC 1275. Note the combination of neutral and ionized species, as discussed in the text.

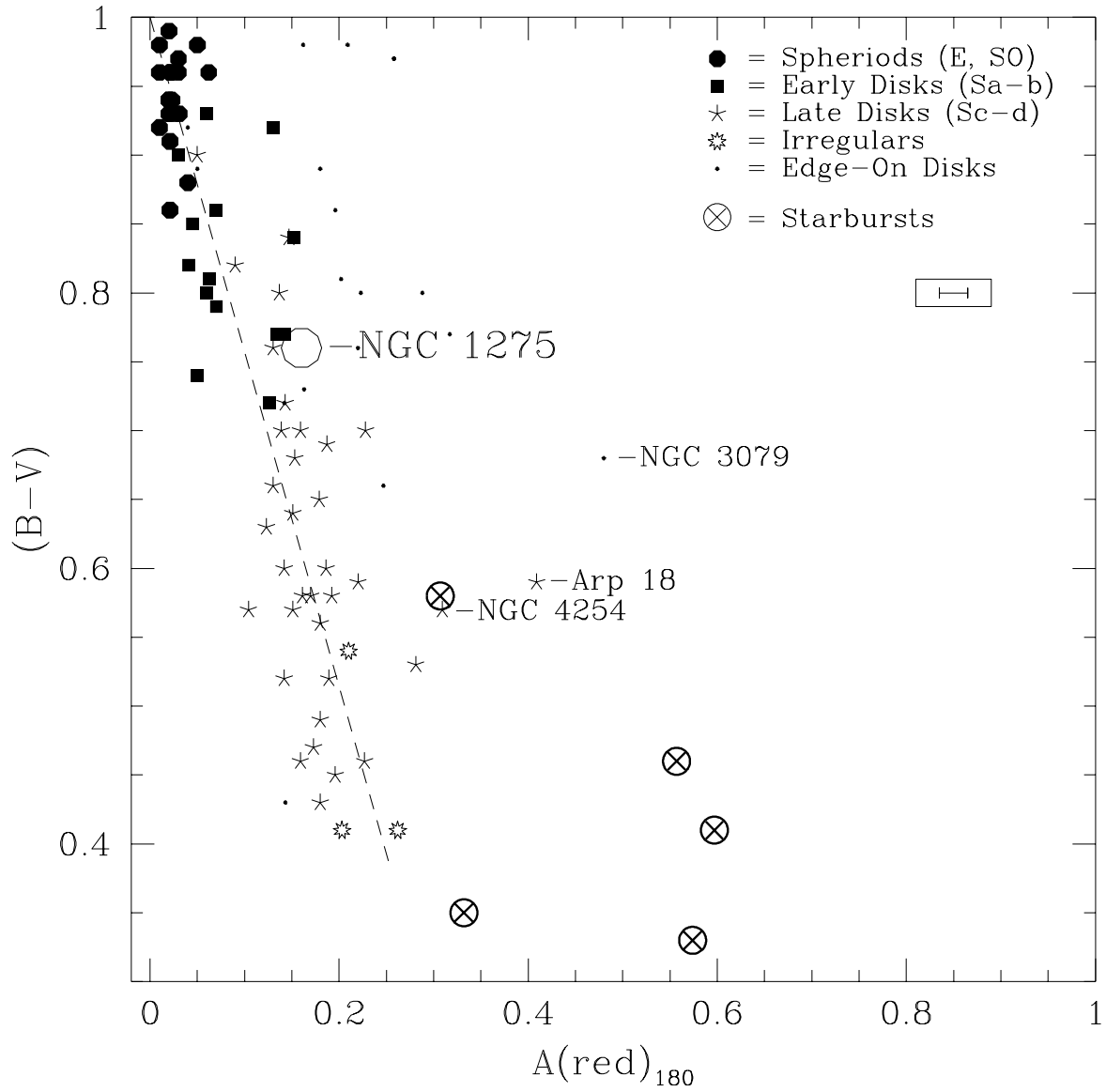


Fig. 13.— Color-Asymmetry Diagram (CAD) for a sample of galaxies, including the position of NGC 1275. This diagram and the ripple features in Figures 8 and 9 reveals that some type of merger took place, probably recently.